Zinc deficiency induces spatially distinct responses in roots and impacts ZIP12-dependent zinc homeostasis in Arabidopsis

Noémie Thiébaut[1,2,3], Daniel Pergament Persson[2], Manon C. M. Sarthou[1], Pauline Stévenne[1], Bernard Bosman[4], Monique Carnol[4], Steven Fanara[1], Nathalie Verbruggen[3], Marc Hanikenne[1]

[1] InBioS-PhytoSystems, Translational Plant Biology, University of Liège, B-4000 Liège, Belgium

[2] Department of Plant and Environmental Sciences, University of Copenhagen, 1871 Frederiksberg, Denmark

[3] Laboratory of Plant Physiology and Molecular Genetics, Université Libre de Bruxelles, 1050 Brussels, Belgium

[4] InBioS-PhytoSystems, Laboratory of Plant and Microbial Ecology, University of Liège, 4000 Liège, Belgium

Corresponding author :

Marc Hanikenne, InBioS – PhytoSystems, University of Liège, Quartier de la Vallée, 1, Chemin de la Vallée, 4 - Bât B22, B4000 Liège, Belgium, email: marc.hanikenne@uliege.be, Tel: +32-4-3663844

.

Abstract

How zinc (Zn) deficiency shapes root development remains unclear, with conflicting reports on its effect on primary root growth in *Arabidopsis thaliana* (Arabidopsis). The impact of Zn shortage on the root apical meristem (RAM) in particular has not been systematically explored. Using an integrative approach combining cell biology, transcriptomics, and ionomics, we dissected how Zn deficiency alters root zonation and function. We showed that Zn deficiency triggers a striking reorganization of the root tip (RT): the RAM size is reduced, yet meristematic activity and local Zn levels are preserved. This is accompanied by promoted cell elongation and differentiation. Transcriptome profiling revealed a distinct Zn deficiency response in the RAM-enriched RT compared to mature root tissues, with *ZIP12* emerging as the most strongly induced gene in the RT. Functional analysis of *zip12* mutants uncovered major defects in root growth, RAM structure, expression of Zn-responsive genes, and metal partitioning. Our work unveiled a new layer of root developmental plasticity under Zn deficiency and identified *ZIP12* as a central player in maintaining Zn homeostasis and root meristem function in *Arabidopsis*. These findings provide a framework to better understand how plants adapt root growth to fluctuating micronutrient availability.

Keywords

Zinc, deficiency, *Arabidopsis thaliana*, root apical meristem, ZIP12, cell cycle, manganese, Laser Ablation ICP-MS

Introduction

Low zinc (Zn) availability in soil is one of the many challenges faced by plants in large natural and agricultural areas worldwide. The resulting Zn deficiency has severe consequences for human health, particularly in countries with a predominantly plant-based diet (Wessells & Brown, 2012; Assunção, 2022). Zn deficiency reduces plant growth as well as crop production and nutritional quality (Alloway, 2008; Thiébaut & Hanikenne, 2022; Lilay *et al.*, 2024), and severely impacts the capacity of plants to respond to other stresses such as drought (Cakmak & Kutman, 2018; Noulas *et al.*, 2018; Hassan *et al.*, 2020), pathogen (Cakmak *et al.*, 2000; Martos *et al.*, 2016; Cabot *et al.*, 2019) high light (Cakmak *et al.*, 2000; Lilay *et al.*, 2024), or exposure to toxic ions (Cakmak *et al.*, 2000). Consequently, Zn deficiency exacerbates other global agricultural challenges. Indeed, it has pleiotropic effects on plants, ranging from imbalance in hormonal regulation, redox status or ion homeostasis, to reduced photosynthetic efficiency, increased light sensitivity and stunted growth (see Lilay *et al.*, (2024) for a recent review).

Among dicots, the response to Zn deficiency is best described in the model plant *Arabidopsis thaliana* (Arabidopsis) (Lilay *et al.*, 2019; Amini *et al.*, 2022; Stanton *et al.*, 2022; Assunção *et al.*, 2022; Thiébaut & Hanikenne, 2022). Zn sensing and regulation are mediated by the bZIP19 and bZIP23 (basic leucine zipper) transcription factors, which trigger a massive induction of genes encoding zinc-regulated/iron-regulated-transporter-like proteins (ZIP) and nicotianamine synthases (NAS) under Zn deficiency (Assunção *et al.*, 2010; Lilay *et al.*, 2019, 2021; Assunção, 2022). Several ZIP transporters were shown to contribute to enhanced Zn uptake by roots, Zn radial transport in roots, and Zn root-to-shoot translocation (Talke *et al.*, 2006; Lin *et al.*, 2009; Ochoa Tufiño *et al.*, 2025). Additionally, nicotianamine (NA) contributes to Zn root-to-shoot translocation by improving radial Zn transport in roots and Zn movement in the xylem (Clemens, 2019). Apart from Zn sensing in roots by bZIP19 and bZIP23, the Zn deficiency response is also regulated by yet-to-be identified shoot signalling (Sinclair *et al.*, 2018). Moreover, Zn deficiency affects the homeostasis of other nutrients. For instance, the Zn deficiency response may lead to an increase of iron (Fe) concentration in plant tissues, caused by (i) the broad metal specificity of transporters, such as ZIPs, and (ii) the high affinity of ligands such as NA for several transition metals (Cakmak, 2000; Milner *et al.*, 2013; Clemens, 2019; Thiébaut & Hanikenne, 2022).

Research and breeding efforts have mostly addressed Zn uptake and homeostasis mechanisms as a main focus to tackle Zn deficiency-related challenges (Garcia-Oliveira *et al.*, 2018; Thiébaut & Hanikenne, 2022; Assunção, 2022; Robe & Barberon, 2023; Huizinga *et al.*, 2025). The broader impact of Zn deficiency on other important plant traits has, however, been largely neglected, although they may be beneficial for coping with additional stresses in the context of global change (Lynch *et al.*, 2021; Lynch, 2022; Lilay *et al.*, 2024). Hence, reduced root growth is a hallmark phenotypic consequence of stress in plants. For instance, modifications in root system architecture have been proposed as promising breeding traits for adaptation to drier climate (Varshney *et al.*, 2021; Lynch *et al.*, 2021; Lynch, 2022). Similarly, identifying the determinants of root growth upon Zn deficiency could uncover mechanisms that could mitigate the effects of low Zn availability in soils.

Maintenance of root growth takes place at the root apex and involves regulation of both quiescence and meristematic activity in the root apical meristem (RAM). This includes mitosis, as well as the onset of endocycling (*i.e.* nuclear genome replication in the absence of mitosis), which is concomitant to the entry of the cells in the elongation and differentiation stages of root development (Bhosale *et al.*, 2018). Zinc is fundamental to plant growth, as it is required as cofactor for ~10% of the plant proteome (Ireland & Martin, 2019; Clemens, 2022), including for the structure and activity of several major transcription factor families (Ciftci-Yilmaz & Mittler, 2008; Phukan *et al.*, 2016; Fedotova *et al.*, 2017; Khoso *et al.*, 2022) and other proteins of the core cell cycle machinery (Kipreos & Pagano, 2000; Bochman & Schwacha, 2009; Chanfreau, 2013; Clemens, 2022).

Whereas the impact of excess Zn (and other metals) on the cell cycle in the RAM and more widely on root growth has been described in details (Eekhout *et al.*, 2017; van Dijk *et al.*, 2022; Richtmann *et al.*, 2025; Thiébaut *et al.*, 2025), only a limited number of studies has examined which phases of the cell cycle are affected by Zn deficiency in plants and algae (Falchuk *et al.*, 1975; Francis *et al.*, 1995; Chesters & Petrie, 1999). Using synchronized BY-2 tobacco cells and the unicellular algae *Euglena gracilis,* these studies pointed antagonistically to either the S, G2-M, or G1 phases as limiting steps under Zn deficiency, while refuting Zn importance in other phases (Falchuk *et al.*, 1975; Francis *et al.*, 1995; Chesters & Petrie, 1999). However, recent and comprehensive studies in plants are lacking.

Here, we investigated the impact of Zn deficiency on root morphology and growth of the root apex in Arabidopsis. We showed that Zn deficiency reduced primary root growth and altered the size of the RAM, with a decrease in the number of dividing cells, accompanied by reduced cell elongation and differentiation. The deficiency did not, however, alter the cell cycle progression. Using complementary Zn element bioimaging and transcriptomics approaches, we identified distinct and different Zn deficiency responses in the RAM compared to differentiated roots, with notably a greater ability of the RAM to maintain cellular Zn levels. We further identified *ZIP12* as the most up-regulated ZIP transporter gene in the root tip (RT) upon Zn deficiency. Characterization of the growth and ionomic phenotypes of z*ip12* mutant plants revealed its key role in metal homeostasis upon severe Zn deficiency in Arabidopsis.

Material and methods

Extended method descriptions are provided in the **Methods S1** text, as supporting information.

Plant material, culture media and culture conditions

Arabidopsis thaliana (Col-0) was used in all experiments. The *ZIP12* (*AT5G62160*) mutants [*zip12-1* (SALK_137184), *zip12-2* (SALK_118705)], as well as the pCYCB1;2:CYCB1;2:GUS (N799897) and pCYCA3;1:CYCA3;1:GUS (N799893) lines were obtained from NASC (Nottingham Arabidopsis Stock Centre, UK) (**Fig. S1**, **Table S1**). The following lines were also used: pWOX5:GUS (Sarkar *et al.*, 2007), pZIP4:GUS [BG0011, (Lin *et al.*, 2016)], and *atm-1* (Garcia *et al.*, 2003).

After surface sterilisation (Lindsey *et al.*, 2017), seeds were sown directly on sterile petri plates with 50 mL of EDTA-washed agar Hoagland medium, which contained $ZnSO_4$ in various concentrations (0 µM, 1 µM, 2 µM or 5 µM), as indicated. Growth conditions were as described in Thiébaut *et al*. (2025). Unless otherwise stated, all experiments were conducted in three independent replicates. The replication level of each experiment is detailed in figure legends.

Root growth and RAM phenotyping

Primary root length of two-week-old plantlets was measured on images of scanned plates. Confocal microscopy images of propidium iodide-stained roots were used to measure

the length of meristematic (Perilli & Sabatini, 2010) and elongation zones, as well as the size and number of RAM cortex cells. FIJI (https://imagej.net/Fiji) was used for all measurements.

GUS staining and MUG assay

GUS staining and quantification of pZIP4:GUS, pWOX5:GUS, pCYCA3;1:CYCA3;1:GUS and pCYCB1;2:CYCB1;2:GUS were performed as previously described (Charlier *et al.*, 2015; Thiébaut *et al.*, 2025). The stained plantlets were then imaged with a Nikon SMZ1500 stereomicroscope equipped with a Nikon Digital Sight DS-5M camera (Nikon, Japan). Cell cycle synchronization was achieved using hydroxyurea, as described (Cools *et al.*, 2010).

RNA preparation

For RNA-Seq analysis, each root tip (RT) sample (~2 mm length) was collected from the primary roots of ~650 plantlets (Richtmann *et al.*, 2025; Thiébaut *et al.*, 2025), the remaining roots (RR) were pooled in a second associated sample. Total RNAs were extracted with the Maxwell® RSC Plant RNA Kit (Promega, USA) using a Maxwell® RSC robot (Promega, USA) and quality was controlled on a Bioanalyzer using a QC RNA kit (Agilent Technologies, USA) prior to RNA-Seq library preparation.

For Reverse Transcription-quantitative Polymerase Chain Reaction (RT-qPCR), samples were collected in biological triplicates. Each sample, ~160 plantlets, was ground using a MM200 mixer mill (Retsch, Germany). Total RNA was extracted using the RNAeasy Microkit (Qiagen, Germany).

RT-qPCR

cDNAs were prepared from 300 ng total RNA using Oligo(dT) with the RevertAid H Minus First Strand cDNA Synthesis Kit (Thermofischer, USA). RT-qPCR was conducted in technical triplicates for each 15x-diluted cDNA sample/primer combination with the Takyon Low Rox SYBR MasterMix dTTP Blue kit (Eurogentec, Belgium) on a QuantStudio5 thermocycler (Applied Biosystems, Thermofischer, USA) with the primers listed in **Table S1**. Primer pair efficiency was calculated using the LinReg PCR software (Ramakers *et al.*, 2003) and expression was normalized with the expression of three housekeeping genes [*At5g60390-EF1alpha*, *At4g05320-UBQ10*, and *At1g58050,* (Nouet *et al.*, 2015)] and relative to the control (2 µM Zn) using the qBase+ software (v.3.4.1, Biogazelle, Belgium).

RNA-Seq, library preparation, sequencing, data analysis and representation

Library preparation (from 500 ng total RNA), quality control, quantification and RNA-Sequencing performed on a NovaSeq6000 were conducted at the GIGA Genomics platform of ULiège (Flowcell S4 V1.5, with 2x paired-end reads of 150 nucleotides). Data quality assessment and trimming, read mapping, counting and differential expression analysis were performed as described (Scheepers *et al.*, 2020; Thiébaut *et al.*, 2025).

A manually assembled list of cell cycle marker genes used for analysis is presented in **Table S2**. GO enrichment analysis for biological processes was conducted using the Panther Database (https://pantherdb.org).

Identification of the transcription factors was performed by comparing DEG lists to the *A. thaliana* Transcription Factor DataBase (AtTFDB) from the Arabidopsis Gene Regulatory Information Server (AGRIS, https://agris-knowledgebase.org/AtTFDB/).

Mineral analysis

Shoots and roots of 160-180 two-week-old plantlets per sample were separated, then desorbed and washed (Scheepers *et al.*, 2020; Thiébaut *et al.*, 2025). Dried root and shoot samples were weighted, digested in HNO_3 using a high-temperature digestion block, and analysed by ICP-OES (Inductively Coupled Plasma Optical Emission Spectroscopy, 5100 ICP-OES, Agilent Technologies, USA) (Nouet *et al.*, 2015).

Zinc imaging by Laser Ablation ICP-MS

Roots of two-week-old plantlets were harvested and two samples from the two regions of interest [*i.e.* the RAM (at ~200 µm distance from the tip of the columella) and differentiated roots (at a distance from the root apex corresponding to 50-60 % of the total root length)] were prepared by encapsulation in melted paraffin and then frozen in a block of freezing media, as described (Thiébaut *et al.*, 2025). Fourteen-µm thick sections were prepared (Persson *et al.*, 2016), freeze-dried, photographed and analysed using a LA-ICP-MS system (Laser Ablation Inductively Coupled Plasma Mass Spectrometry).

Results

Zn deficiency impacts root growth

Compared to control growth conditions (1 µM Zn), both shoot and root growth was inhibited in Arabidopsis plantlets that were germinated and grown for 2 weeks on Zn-deprived

192 solid agar medium (*i.e.* without any added Zn, 0 µM Zn) [**Fig. 1a, c-d,** (Thiébaut *et al.*, 2025)].
193 The inhibition of primary root growth was accompanied by a reduction in size of the RAM,
194 measured both in µm and in number of cortical cells present in the division zone (**Fig. 1b, e-f**).
195 Moreover, the cortex cells in the division zone (delimited by the red arrows in **Fig. 1b**) were
196 longer in Zn deficiency-exposed RAM (**Fig. 1b, g**).

197 Additionally, upon Zn deficiency, the elongation of cortex cells was initiated closer to
198 the tip of the root, thus resulting in an increased cortex cell size compared to control roots at
199 the same relative position in the elongation zone (**Fig. 2a**). This difference was striking within
200 the first 250 µm adjacent to the RAM, where the elongation was estimated to be ~2x faster
201 (**Fig. S2**), yielding 2.7 times longer cells at a distance of 500 µm from the QC in Zn deficiency-
202 exposed roots (**Fig. 2a**). In contrast, mature cortex cells were ~13% smaller upon Zn deficiency
203 (**Fig. 2b**). Finally, cell differentiation initiated closer to the tip of the root, as the appearance
204 of the first root hairs was closer to the QC (**Fig. 2c**).

205 Altogether, Zn deficiency had an impact on RAM morphology, potentially affecting
206 three developmental processes: division, elongation and differentiation.

207 Observation of propidium iodide-stained roots did not indicate cell death occurring in
208 RT exposed to Zn deficiency, as the absence of propidium iodide staining inside meristematic
209 cells suggested that plasma membrane integrity was preserved (see Material and Methods,
210 **Fig. 1b**). This observation, however, did not exclude compromised meristematic activity
211 and/or quiescence upon Zn deficiency. In pWOX5:GUS lines, reporting for quiescence
212 maintenance (Sarkar *et al.*, 2007), the intensity and localization of the GUS staining were
213 unaffected by Zn deficiency (**Fig. 3a**), indicating that both the QC identity and function were
214 maintained upon Zn deficiency.

215 Next, the progression of the cell cycle was assessed by exposing
216 pCYCA3;2:CYCA3;2:GUS (S phase reporter) and pCYCB1;2:CYCB1;2:GUS (G2/M phase
217 reporter) lines, both expressing a fusion protein susceptible to post-translational
218 modifications (Cools *et al.*, 2010; Bulankova *et al.*, 2013; Schnittger & De Veylder, 2018), to Zn
219 deficiency (**Fig. 3b-c**). The GUS staining localization was conserved in both lines across all
220 tissues in Zn-deficient RAM, compared to control RAM (**Fig. 3b-c**). However, quantification of
221 the GUS staining revealed that both cell cycle markers were ~30% less expressed in Zn
222 deficiency-exposed roots, suggesting a global effect on cell division in the RAM (**Fig. 3d**).

Despite this observation, computing the Division Rate Index (Perilli & Sabatini, 2010) to assess the effect of Zn deficiency on the division activity of individual cells in the meristem, did not reveal any difference between Zn deficiency and control conditions (**Fig. 3e**). This suggests that individual cells underwent both S and G2/M cell cycle phases at the same rate, in both conditions. The duration of cell cycle phases was further assessed upon hydroxyurea (HU)-induced synchronization, and monitoring of re-entry in S and G2/M phases over 28 hours (**Fig. S3a-b**). In plantlets grown in control conditions, GUS staining peaked at 12-16h (**Fig. S3a**) and 20-24h (**Fig. S3b**) post HU treatment, for S and G2/M phase markers, respectively. At the temporal resolution used in this experiment, no alteration of the timing of S and G2/M phase progressions was observed in plantlets grown in Zn deficiency, although a reduced number of GUS-stained cells was observed at certain timepoints for the G2/M lines (**Fig. S3c**). Altogether, these findings suggested that the reduced RAM size mainly resulted from a reduced number of dividing cells (**Fig. 3b-d**). This was caused either by accelerated elongation rather than from reduced division rate per cell, or by a defect in cell cycle progression within the division zone. Additionally, Zn deficiency led to shorter mature cells (**Fig. 2b**), and differentiation initiating closer to the tip of the root (**Fig. 2c**).

Zinc distribution differs in RAM and differentiated root tissues

Zn distribution in Col-0 root tissues was examined using LA-ICP-MS (Persson *et al.*, 2016; Thiébaut *et al.*, 2025). Transversal sections were acquired across fully differentiated roots and the primary RAM (**Fig. 4).** The ^{39}K distribution was mainly used to verify the integrity of the root sections: it was homogeneous across every cell layer of the root, except for a few cortex cells in the differentiated root sections, which sometimes appeared empty in their centre (**Fig. S4**).

In control conditions, the ^{66}Zn distribution peaked in the vascular cylinder of differentiated roots (**Fig. 4a**).The ^{66}Zn signal was higher in the RAM than in differentiated roots, with a more homogenous distribution across all cell layers and a slight tendency for higher ^{66}Zn accumulation in the epidermis [**Fig. 4b,** (Thiébaut *et al.*, 2025)]. Upon Zn deficiency, ^{66}Zn levels strongly decreased across differentiated roots (**Fig. 4a,c**). In contrast, ^{66}Zn was maintained in the RAM, at levels similar to those of the control condition (**Fig. 4b**). Zn depletion seemed to progress centripetally across cell layers, with a slightly decreasing ^{66}Zn

concentration in the epidermis, but with conserved Zn level across the other tissues of the RAM (**Fig. 4b,d**). Interestingly, the ability of the RAM to maintain cellular Zn levels mirrored the maintained meristematic activity upon Zn deficiency.

Root tip and remaining root display distinct transcriptomic responses to Zn deficiency

To capture the impact of Zn deficiency on root tip (RT) processes, including distinct Zn homeostasis, the transcriptional response of the RT to Zn deficiency relative to the remaining root (RR) system was examined by RNA-Seq analysis (Richtmann *et al.*, 2025; Thiébaut *et al.*, 2025). Again, Arabidopsis plantlets were germinated and grown for two weeks on control (1 µM Zn) or Zn-deprived (0 µM Zn) agar medium. At harvest, RT (~2 mm from the tip of the root, including columella, RAM and elongation zone) of the primary roots were separated from the RR, prior to sample preparation and RNA-Seq analysis.

In agreement with previous studies using the same experimental design (Richtmann *et al.*, 2025; Thiébaut *et al.*, 2025), the root part (RT vs RR) explained ~90% of the variance in gene expression, whereas the Zn deficiency treatment explained ~7% of this variance (**Fig. 5a**). Accordingly, 2530 and 3595 differentially expressed genes [DEGs, $\log_2$ (fold change) < -1 of > 1; adjusted *p-value* < 0.05] were identified between RT and RR, in control and Zn deficiency conditions, respectively (**Fig. 5b-c, Table S3**). Among those, 1825 were common to both growth conditions. The DEGs between RT and RR represented a vast range of functions according to Gene Ontology (GO) enrichment analysis [*e.g.* cell wall biogenesis and modification, root hair differentiation, cell growth or nucleic acid synthesis and transcription] (**Tables S4**, **S5**).

Furthermore, detailed analysis revealed distinct responses of the two root parts (RT and RR) to Zn deficiency, with only partially overlapping sets of DEGs (**Fig. 5d-e**). For instance, only 2 of the top 10 upregulated DEGs in RT upon Zn deficiency were also differentially expressed in RR (**Table 1**). Moreover, a majority of DEGs were up-regulated upon Zn deficiency in the RT (525 up vs 65 down), whereas the opposite trend was observed in the RR (249 down vs 197 up) (**Fig. 5d-e**, **Table S6**). GO enrichment analysis identified a wide diversity of up- or down-regulated processes in RT and RR upon Zn deficiency (**Fig. 5f-g**).

Among the genes up-regulated by Zn deficiency in RT and RR, several over-represented GO categories were related to biotic stress responses and to interactions between organisms

(**Fig. 5f-g**). Most of them were also associated with hormonal response GOs, response to hypoxia and/or to oxygen compound GOs, all belonging to general regulatory pathways, or to the response to diverse abiotic stresses including metal imbalance (Remans *et al.*, 2012; Huang *et al.*, 2019; Scheepers *et al.*, 2020; Yaqoob *et al.*, 2022; Thiébaut *et al.*, 2025), suggesting common signalling of those responses.

The GO enrichment analysis further indicated that development biological processes were differentially affected by Zn deficiency in RT and RR (**Fig. 5f-g**). In RT, cell wall biogenesis and root system development were over-represented among the Zn deficiency up-regulated DEGs, while GOs associated to gene expression and RNA metabolic processes were under-represented in the same group of genes. Accordingly, among the top regulated genes in the Zn-deficient RT were found genes involved in cell wall differentiation (*XTH26*), and in the control of root development (*PILS7*, *ESE2, WRKY1*, *EIL2*) [**Table 1**, (Wang *et al.*, 2007; Somssich *et al.*, 2016; Wu *et al.*, 2022)]. In RR, a mirrored situation was observed: root developmental processes and cell differentiation were over-represented among Zn deficiency down-regulated DEGs, while GOs associated to gene expression were under-represented in the same group of genes (**Fig. 5f-g**).

In the RT, Zn deficiency also led to the upregulation of several DEGs related to ion transport and nutrition, including enriched GOs related to phosphate (Pi) and Zn homeostasis (**Fig. 5f**). Hence, *ZIP12*, encoding a putative Zn transporter (Milner *et al.*, 2013), was the top upregulated gene in RT upon Zn deficiency, and a defensin-like (DEFL208)-encoding gene which was recently linked to the impact of Zn deficiency on root growth (Kimura *et al.*, 2023) was also strongly up-regulated in RT (**Table 1**). Moreover, actors involved in Fe homeostasis regulation (*bHLH38*, *WRKY12*) as well as Fe transport (*IRT2*, *VIT-like*) were found among the DEGs in the RT upon Zn deficiency (**Tables 1**, **S6**). Surprisingly, no enrichment for Zn homeostasis GOs was observed among the DEGs in the RR upon Zn deficiency (**Fig. 5f**).

Finally, top up- and down-regulated genes in RT upon Zn deficiency also included several poorly annotated and characterized genes, among them genes encoding putative kinases and transmembrane or transporter proteins (**Table 1**).

The impact of Zn deficiency on the cell cycle and root development is reflected in the transcriptome

Root development was affected by Zn deficiency, as observed at both phenotypic (**Fig. 1-3**) and transcriptional levels with enriched development and differentiation GOs (**Fig. 5**). Root growth and development depend on cell division, but also on cell cycle exit into elongation and differentiation, often accompanied by endoreduplication (Veylder *et al.*, 2011; Braidwood *et al.*, 2014; Bhosale *et al.*, 2018; Shen *et al.*, 2025).

Although a reduced number of dividing cells was observed in the RAM upon Zn deficiency (**Fig. 3**), cell cycle processes were hardly represented among Zn deficiency-induced DEGs (**Fig. 5f-g**, **Tables 1**, **S6**). Nevertheless, hierarchical clustering of a manually curated list of cell cycle, endocycle and DNA damage response (DDR) genes (125 genes, **Table S2**, **Fig. S5a-c**) indicated (i) an overall decreased expression of endocycle and S phase genes in RR compared to RT, (ii) a decreased expression of G2/M phase genes in RT, and increased expression of DDR genes in RT and RR upon Zn deficiency, respectively (**Fig. S5**). Interestingly, root growth was negatively impacted by Zn deficiency in an *atm-1* (*ataxia telangiectasia mutated*) mutant, defective in DDR signalling (Garcia *et al.*, 2003) (**Fig. S5d**).

The impact of Zn deficiency on the cell cycle was confirmed by cross-referencing Zn deficiency DEGs with a set of genes specifically expressed at the different phases of mitosis or during endoreduplication (which is linked to the onset of elongation) (**Fig. S6a**, **Table S7 Sheets 1-2**), as identified by single-cell (sc)RNA-Seq (Torii *et al.*, 2020). This comparison showed an enrichment of 104 “G1-endocycle” genes specifically among the 525 DEGs up-regulated in RT upon Zn deficiency, (representing 24% of the scRNA-Seq cluster specific to this phase), mirrored by an increase of the down-regulated DEGs in RR upon Zn deficiency (**Fig. S6a,** underlined in **Table S7 Sheets 1-2**). This indicated a shift of the G1 endoreduplication gene expression from RR to RT upon Zn deficiency, which corroborated the morphological analysis marked by a shortening of the division and elongation zones (**Figs. 1**-**2**).

Finally, to further describe how Zn deficiency affects specific root cell layers, DEGs between RT and RR samples under both control and Zn deficiency conditions were compared with cell type-specific gene expression clusters from a publicly available Arabidopsis scRNA-Seq dataset. This dataset, created by Shahan *et al*. (2022), covers three developmental stages: meristematic, elongating or differentiating (**Table S7 Sheets 3-4, Fig. S6b**). The analysis

showed that the elongation and differentiation gene clusters were more prominently represented in the RT at 0 µM Zn (orange curves) than at 1 µM Zn (green curves) in several cell types, specifically, in trichoblast, cortex and endodermis cells (**Fig. S6b**). These findings suggested that Zn deficiency accelerated elongation and differentiation of different RT cell layers at the molecular level. Specifically, out of the 1166 DEGs with higher expression in RT than in RR solely upon Zn deficiency (**Fig. 5b**), 444 were markers of the elongation and differentiation [(Shahan *et al.*, 2022) (underlined in **Table S7 Sheets 3-4**)**]**.

Zn transporter genes are induced in the root tip upon severe Zn deficiency

Arabidopsis roots typically respond to Zn deficiency through the bZIP19 and bZIP23-mediated massive induction of several ZIP transporter and NAS-encoding genes (van de Mortel *et al.*, 2006; Assunção *et al.*, 2010; Sinclair & Krämer, 2012; Lilay *et al.*, 2021; Thiébaut & Hanikenne, 2022). Several of these genes displayed increased expression in RR and in RT upon Zn deficiency, except for *ZIP10* which displayed almost no expression (**Fig. 6a**). However, only *ZIP12* passed the $\log_2$ (fold change) > 1 and 0.05 *p-value* thresholds in both RR and RT, whereas several additional bZIP19/bZIP23 target genes (*ZIP9*, *ZIP4*, *ZIP1*, *NAS4*) passed these thresholds solely in RT and not in RR (**Figs. 6a, S7a**). At closer inspection, these genes displayed an unusually high expression in control conditions (1 µM Zn), ranking them among the most expressed genes (**Fig. S7b**), and yet still displayed an increased expression upon Zn deficiency (0 µM Zn) in RT.

Growing Col-0 plantlets across an increasing Zn concentration range (0-5 µM Zn) showed that root and shoot growth was reduced at 1 µM Zn compared to 2 and 5 µM Zn, with even greater inhibition at 0 µM Zn (**Fig. 6b**). At 2 µM Zn, several *ZIP* genes were significantly less expressed in roots, as expected for Zn sufficient conditions, compared to 0 µM Zn (**Fig. S7c**). Similarly, when growing a Zn deficiency reporter line [pZIP4:GUS, (Assunção *et al.*, 2010)], GUS staining was observed in roots of plantlets grown at 1 µM Zn but not at 2 or 5 µM Zn (**Fig. 6c**). A more intense GUS staining was however observed at 0 µM Zn, particularly in the vicinity of the RAM, compared to the 1 µM Zn condition.

Agar is a source of metal nutrients (Gruber *et al.*, 2013) and to achieve effective Zn deficiency in agar-based media, Zn traces must be removed, typically by washing the agar with EDTA (Sinclair & Krämer, 2012). Our observations (**Figs. 6, S7**) indicated that the plantlets

grown under our initial control conditions (Hoagland media with 1 µM Zn in EDTA-washed agar) already displayed a Zn deficiency response, that was further induced at 0 µM Zn, particularly in the RT. Therefore, the 1 µM Zn condition may rather be referred to as Zn limitation (Moseley *et al.*, 2002; Esteves *et al.*, 2023), and 0 µM Zn as Zn deficiency. Practically, it suggested that the root morphological features and gene expression patterns reported here at 0 µM Zn compared to 1 µM Zn were those associated with a severe Zn deficiency. In follow-up experiments, 2 µM Zn was used as control, Zn replete, condition.

ZIP12 plays a key role in the Zn deficiency response

Being very poorly expressed in control conditions, *ZIP12* was the most strongly up-regulated gene in RT (log_2 FC = 11.8) and the 4th in RR (log_2 FC = 7.3) upon Zn deficiency (**Tables 1**, **S6**, **Fig. 6a**). *ZIP12* encodes a putative Zn transporter, as determined by yeast complementation assays (Milner *et al.*, 2013) and is a target of the bZIP19 and bZIP23 TFs (Assunção *et al.*, 2010). To further examine the function of *ZIP12* in Zn homeostasis, two *zip12* T-DNA insertion mutant lines, *zip12-1* (SALK_137184) and *zip12-2* (SALK_118705) (Inaba *et al.*, 2015), were phenotyped in Zn deficient conditions (**Figs. 7**, **S1a**). A greater inhibition of the primary root growth upon Zn deficiency was observed in *zip12-1* compared to Col-0 and *zip12-2* (**Figs. 7a, S1b-c**). These phenotypes correlated with the *ZIP12* expression level in the roots of the 3 genotypes upon Zn deficiency, with a strong induction in Col-0 and *zip12-2*, and no expression in *zip12-1* (**Fig. 7b, d**).This suggested that the T-DNA insertion in the *ZIP12* promoter region upstream of the two ZDREs in the *zip12-2* mutant (**Fig. S1a**) did not knock-out its transcription upon Zn deficiency. Therefore, phenotyping was pursued solely with the *zip12-1* mutant. No difference in RAM size was observed between Col-0 and *zip12-1,* but the RAM cortex cells were significantly longer in *zip12-1* compared to Col-0 upon Zn deficiency (**Fig. 7c**).

In *zip12-1*, the absence of *ZIP12* transcripts was compensated by higher expression of other *ZIP* genes (*IRT3*, *ZIP3*, *ZIP4*, *ZIP9*) in control conditions (2 µM Zn) compared to Col-0, reaching levels close to their peak expression in Zn deficiency (**Fig. 7d**). Zn accumulation in whole roots and shoot of *zip12-1* varied only marginally from Col-0 both in control and Zn-deficient conditions (**Fig. 7e**). In contrast, under control conditions, *zip12-1* accumulated 1.5 and 2.2 times more Mn and Cu in shoots, and 1.85 times more Mn in roots compared to Col-0

(**Fig. 7e**). Upon Zn deficiency, Cu levels in *zip12-1* shoots decreased to Col-0 concentrations, while Mn accumulation in *zip12-1* roots and shoots was strongly reduced, by 10.78x and 2.60x, respectively, and was below Col-0 concentrations. The shoot and root concentrations of all other elements measured (Ca, Fe, K, P, Mg, Na) remained unaffected by the genotype or the treatment, except for Mg in roots, which was reduced by Zn deficiency in both Col-0 and *zip12-1* (**Fig. S8**).

The ^{66}Zn distribution in *zip12-1* root tissue sections, examined using LA-ICP-MS, revealed a similar pattern to that of Col-0: upon Zn deficiency, ^{66}Zn levels were strongly reduced in differentiated roots, particularly in the vascular cylinder, whereas they were maintained in the RAM (**Fig. 4**). However, two noticeable differences in the ^{66}Zn distribution were observed between the *zip12-1* mutant and Col-0. First, in control conditions, *zip12-1* displayed higher ^{66}Zn levels in the vascular cylinder than Col-0. Second, the centripetal decrease in Zn level from the epidermis towards the root centre observed in Col-0 was more marked in the RAM of *zip12-1* (**Fig. 4**).

Discussion

Root growth and architecture are strongly influenced by nutrient availability, as are the RAM morphology and activity. Low nutrient availability can ultimately result in total exhaustion of quiescence and meristematic activity in the RAM (Ward *et al.*, 2008; Jain *et al.*, 2009; Lequeux *et al.*, 2010; Gruber *et al.*, 2013; Bouain *et al.*, 2019). Here, we showed that severe Zn deficiency resulted in strongly impaired primary root growth and altered RAM morphology, with (i) shortened division zone, while quiescence was maintained and individual cells retained meristematic activity, (ii) shortened elongation zone made of longer cells, and (iii) accelerated differentiation resulting in shorter mature cells (**Fig. 8**). Zn was homogenously distributed in the RAM, and this distribution was maintained upon severe Zn deficiency, in contrast to RR. Finally, our data indicated an important role of the ZIP12 transporter in the response to Zn deficiency (**Fig. 8**). Altogether, our results suggested that, despite a reduction of its size and of overall root length, the RAM was actively protected from becoming Zn deficient, possibly through prioritised Zn allocation and/or retention.

Zn deficiency alters RAM function and root zonation through multiple, interconnected mechanisms

In Arabidopsis, RAM size reduction is a common response to both nutrient deficiency and toxicity (Sánchez-Calderón *et al.*, 2005; Wei *et al.*, 2021; van Dijk *et al.*, 2022; Thiébaut *et al.*, 2025). Although RAM size, overall cell number and meristematic activity were reduced (**Figs. 1-3, 8**, **S2**), quiescence and division at the single cell level persisted, with no sign of cell death (**Figs. 1, 3, S3**). This was consistent with the observation that Zn levels in the RAM remained relatively stable under Zn deficiency (**Figs. 4, 8**). At the transcriptomic level, Zn deficiency had limited impact on core cell cycle gene expression (**Fig. S5a-c**). However, regulation of the cell cycle, for instance upon stress, is mainly a post-transcriptional process (Marrocco *et al.*, 2010; Genschik *et al.*, 2014; Hu *et al.*, 2016; Velappan *et al.*, 2017), which may account for the observed reduction in meristem activity.

Several processes are known to contribute to RAM size in stress conditions, including for instance DDR, cytoskeletal dynamics and hormonal signalling (Lipka & Müller, 2014; van Dijk *et al.*, 2022; Shi *et al.*, 2023). Several of these processes were impacted by Zn deficiency, as outlined below.

First, DDR pathways are known to mediate cell cycle arrest and RAM size reduction in response to stresses such as Pi deficiency or aluminium toxicity (Sánchez-Calderón *et al.*, 2005; Wei *et al.*, 2021). In this study, Zn deficiency did not induce cell death but did increase the expression of DDR-related genes, both in the RT and RR (**Fig. S5a-c**). Notably, an *atm* mutant, lacking a key DDR kinase, exhibited heightened sensitivity to Zn deficiency, with reduced root growth (**Fig. S5d**). The ATM kinase mediates S and G2 phases arrest and DNA repair, enabling genome protection under stress (Kurz & Lees-Miller, 2004; Nisa *et al.*, 2019). This suggested that ATM may play a role in maintaining root growth under Zn deficiency conditions by enabling a protective DDR and RAM size control.

Second, Zn deficiency increased cell size within the RAM, which is a rather uncommon phenotype under nutrient stress. In Arabidopsis, metal stress-related cell expansion in the RAM was previously described upon Ni excess (Lešková *et al.*, 2020) and in the Cu-sensitive *copper modified resistance1/patronus1* (*cmr1/pans1*) mutant (Juraniec *et al.*, 2016). In both cases, the large cell phenotypes were linked to altered microtubule dynamics. Since Zn promotes microtubule polymerization (Hesketh, 1982; Oteiza *et al.*, 1990), Zn deficiency may

alter microtubule homeostasis in the RT, leading to cell expansion. This hypothesis merits further investigation. Alternatively, endoreduplication is known to contribute to cell expansion via cell wall remodelling (Takahashi, 2013; Bhosale *et al.*, 2018) The higher expression of endoreduplication genes observed in the RT upon Zn deficiency (**Fig. S6a, Table S7 Sheets 1-2**) may possibly drive cell expansion in our experimental conditions.

Third, root zonation, *i.e.* the delineation of the division, elongation and differentiation zones in the RT, is tightly controlled. Here, using the Shahan *et al.* (2022) scRNA-Seq dataset, which provides cell type-specific gene expression clusters across different developmental stages, we showed that under Zn deficiency conditions, markers of elongation and differentiation were more prevalent in RT compared to Zn control conditions. This suggested an acceleration of elongation and differentiation (**Fig. S6b, Table S7 Sheets 2-4**). These processes are tightly regulated by hormonal signals (Tsukagoshi *et al.*, 2010; Takahashi, 2013; Bhosale *et al.*, 2018; Zluhan-Martínez *et al.*, 2021). In particular, opposite auxin and cytokinin (CK) gradients are known to regulate the exit of cell cycle and thus the transition from division to elongation and differentiation zones (Chapman & Estelle, 2009; Tsukagoshi *et al.*, 2010; Kong *et al.*, 2018; Bhosale *et al.*, 2018). Zn deficiency generally decreases auxin levels in dicot roots (Thiébaut & Hanikenne, 2022; Lilay *et al.*, 2024), and genes involved in auxin signalling have been linked to Zn homeostasis in maize (Xu *et al.*, 2022; Wang *et al.*, 2023). In parallel, CK are also associated to the control of Zn homeostasis (Gao *et al.*, 2019). In our dataset, auxin and CK signalling genes showed only moderate changes in expression, with the notable exception of the downregulation of *ARR15* (log_2(FC) -3.52, **Table S6**), a repressor of CK signalling (Kiba *et al.*, 2003). Since CK is known to promote elongation-related processes such as endocycling and cell-wall synthesis, to the detriment of cell cycle activity, meristematic cell number and RAM size (Takahashi *et al.*, 2013; Takahashi & Umeda, 2014; Liu *et al.*, 2022), the repression of *ARR15* upon Zn deficiency may enhance these CK-mediated processes and thereby potentially contribute to RAM shortening. In addition, ethylene is a key regulator of root development, particularly of root hair formation (Zluhan-Martínez *et al.*, 2021; Martin *et al.*, 2022). In this study, we observed that upon Zn deficiency, root hairs initiated closer to the RAM (**Fig. 1, 2, 8**), which is a hallmark of altered root zonation. Moreover, two ethylene-responsive transcription factors, *ESE2* and *EIL2*, were among the most strongly up-regulated TFs (log_2 FC 5.91 and 4.89, respectively; **Table 1**). These findings support the hypothesis of a

role for ethylene signalling in the Zn deficiency response, which is consistent with its involvement in other nutrient stresses (Barberon *et al.*, 2016; Gutiérrez-Alanís *et al.*, 2017; García *et al.*, 2021)

Finally, the *DEFL202, 203, 207,* and *208* genes were strongly upregulated in the RT upon Zn deficiency (**Table 1, Table S6**). Defensin-like (DEFL) peptides, which are small cysteine-rich peptides known for their role in various biotic and abiotic stress responses (Stotz *et al.*, 2009; Wu *et al.*, 2016; Domingo *et al.*, 2024), are additional candidates for a potential role in RAM size regulation. DEFL-encoding genes were described as part of the Zn deficiency response, possibly via the action of bZIP19 (Inaba *et al.*, 2015; Kimura *et al.*, 2023). Notably, a *defl202/203* double mutant exhibits longer RAM and primary root in Zn-sufficient conditions. Although the underlying mechanism of action remains unclear, DEFL peptides have been proposed to limit the RAM size as a strategy to conserve Zn resources in the RAM under low Zn availability. However, the *bzip19/23* double mutant, even though deficient in *DEFL* induction, shows shorter roots under Zn deficiency (Lilay *et al.*, 2019), possibly due to impaired Zn allocation and early RAM exhaustion.

Zn concentration is maintained in the RAM during Zn deficiency

In differentiated roots of Arabidopsis plants grown in control conditions (2 µM Zn), Zn was mostly concentrated in the vascular cylinder (**Fig. 4a, c**). This is consistent with the fact that xylem loading is key for Zn translocation to the shoot (Hussain *et al.*, 2004; Sinclair *et al.*, 2007) and is considered as a bottleneck for Zn translocation to the shoot (Claus *et al.*, 2013; Kisko *et al.*, 2018). In contrast, Zn was homogeneously distributed in the RAM, accumulating at concentration approximately ~10-fold higher than in differentiated roots (**Fig. 4b, d,** (Ochoa Tufiño *et al.*, 2025; Thiébaut *et al.*, 2025), likely reflecting the primary role of Zn in active cell division (Falchuk *et al.*, 1975; Francis *et al.*, 1995). Despite the low expression of genes encoding ZIP transporters, considered as the primary Zn uptake system in Arabidopsis roots, in Zn sufficient condition [**Fig. S7**, (van de Mortel *et al.*, 2006; Ochoa Tufiño *et al.*, 2025)], the Zn enrichment in the RT suggested that Zn may be more efficiently taken up, retained in and/or actively translocated to the meristem. The higher Zn levels in future epidermal cells in the RAM further support a role for Zn uptake in shaping the Zn distribution pattern in the meristematic zone (**Figs. 4, 8**). Recently, *IRT3* and *YSL3* were shown to be expressed upon Zn

deficiency in the division zone, whereas *ZIP3* and *ZIP5*, involved in Zn uptake, were expressed in epidermis cells of the elongation zone (Ochoa Tufiño *et al.*, 2025).

Upon Zn deficiency, Zn levels dramatically decreased in differentiated roots (**Fig. 4a, c**). The gradual upregulation of *ZIP* genes when roots are exposed to Zn sufficiency (2 µM Zn), Zn limitation (1 µM Zn) or severe Zn deficiency (0 µM) (**Figs. 6, S7**) appeared to be insufficient to maintain Zn homeostasis when Zn supply was severely low. Such a gradual and fine-tuned response to Zn deficiency may explain the fact that Zn deficiency has been reported to have either a negative (Talukdar & Aarts, 2008; Mager *et al.*, 2018; Kimura *et al.*, 2023), a positive (Sinclair & Krämer, 2012; Lilay *et al.*, 2019), or no visible (Assunção *et al.*, 2010; Gruber *et al.*, 2013) effect on primary root growth in Arabidopsis. These apparent inconsistencies among previous reports are likely linked to how much Zn traces remained in the growth medium and thus to the severity of Zn deficiency applied in the different experimental systems. The different growth media included the use of different agar powders (Jain *et al.*, 2009; Gruber *et al.*, 2013), either washed with EDTA, or not (Sinclair & Krämer, 2012; Charlier *et al.*, 2015). Here, we observed that a control growth medium made of Hoagland with 1 µM Zn and EDTA-washed agar (i.e. with reduced Zn contamination) was not a Zn sufficient condition, resulting in Zn limitation, *i.e.* an intermediate state where root growth was only moderately affected, but where the bZIP19/bZIP23-dependent molecular response to Zn deficiency was activated already. Such a gradual response was previously reported in the alga Chlamydomonas, where the response to Fe deficiency progressed from an induction of uptake to a massive metabolic reorganization as the Fe supply was gradually decreased (Moseley *et al.*, 2002; Urzica *et al.*, 2012).

In contrast to RR, Zn levels were essentially maintained in the RAM in Zn deficiency conditions (0 µM Zn), as shown both by Zn imaging in the RAM (**Figs. 4b, d, 8**) and by the limited upregulation of *ZIP* genes in Zn-limiting conditions (1 µM Zn) (**Fig. 6a**). Such prioritized Zn allocation to the RT possibly preserved the meristematic activity. Several hypotheses can be formulated to interpret this observation. First, strong upregulation of several *ZIP* genes in the RT upon Zn deficiency [**Figs. 6**, **S7**, (Ochoa Tufiño *et al.*, 2025)] could contribute to stronger Zn uptake and Zn distribution between cell layers. For instance, the strong increase of *pZIP4:GUS* expression in the vicinity of the RAM was striking. Despite this strong induction of Zn transport, Zn depletion was visible in the most external cell layer of the RAM, suggesting

that the Zn homeostatic mechanisms were also starting to be overcome. Second, the densely organized meristem, composed of smaller cells with a reduced vacuolar lumen and thus more concentrated enzymes, molecules and cell-walls than differentiated roots, may act as a Zn sink, contributing to higher Zn concentrations in the RAM. Lastly, as observed for Pi homeostasis (Kanno *et al.*, 2016), the entire root system could contribute to Zn uptake, which would then be translocated to the RAM.

Finally, in two separate studies, we observed reduced Zn and cadmium (Cd) accumulation in the Arabidopsis RAM compared to differentiated tissues upon Zn excess (Thiébaut *et al.*, 2025) or Cd exposure (Richtmann *et al.*, 2025), respectively. Combined, these observations indicate that Zn homeostasis in the RAM is maintained over a wider range of external Zn supply than in differentiated tissues, prioritizing Zn allocation to the RAM upon Zn deficiency or protection of the RAM upon Zn excess (or Cd exposure). This mobilizes a specific response of Zn homeostasis genes (including *ZIP12* upon Zn deficiency, see below), but also of the homeostasis of other nutrients, such as Fe or Pi, of the specialized metabolism, of cell wall modification processes and/or of developmental processes (this study; Richtmann *et al.*, 2025; Thiébaut *et al.*, 2025).

The interaction between Zn and Pi homeostasis also takes place in the RT

The crosstalk between Zn and Pi homeostasis is well documented. In Arabidopsis, low Pi supply increases shoot Zn accumulation, whereas Zn deficiency induces Pi uptake (Khan *et al.*, 2014; Kisko *et al.*, 2018). In line with this interplay, we observed that Zn deficiency induced the expression of Pi-related genes in the RT. These include two genes encoding Pi transporters (*PHO1;H1* and *PHT3;2*) and three members of the Pi starvation-induced glycerol-3-phosphate permease gene family (*G3Pp1-3*) (**Table S6**). Additionally, *ZAT6*, a gene previously shown to be up-regulated during Pi starvation (Devaiah *et al.*, 2007), was also induced in RT upon Zn deficiency (**Table 1**). The ZAT6 TF controls root development and multiple stress responses, including response to Cd exposure, acting on the redox status (Chen *et al.*, 2016; Tang & Luo, 2018). Interestingly, *PHT1;1*, a gene encoding a major contributor in Pi uptake upon Zn deficiency (Ayadi *et al.*, 2015; Rai *et al.*, 2015), was not identified among DEGs in the RT (**Table S6**). Finally, *PILS7* (*PIN-LIKES7*), encoding a putative auxin transporter, was strongly upregulated in RT upon Zn deficiency (Log_2 FC 8.2, **Table 1**). PILS7 has previously been shown

to control root growth in response to Pi supply, and other stress conditions (Yi *et al.*, 2021) suggesting it may also contribute to the Zn deficiency response.

ZIP12 acts a last resort ZIP transporter upon Zn deficiency

The induction of *ZIP* gene expression is a hallmark of the Zn deficiency response in plants (Talke *et al.*, 2006; van de Mortel *et al.*, 2006; Assunção *et al.*, 2010; Dong *et al.*, 2018; Amini *et al.*, 2022; Thiébaut & Hanikenne, 2022). In this study, several *ZIP* genes were strongly up-regulated in the RT upon Zn deficiency (**Figs. 6a**, **S7**). Among them, *ZIP12* was the most up-regulated gene in the RT. The ZIP12 transporter is a putative Zn transporter, as it was shown to complement a Zn uptake-impaired yeast mutant, but did not appear to transport other metals such as Mn or Fe (Milner *et al.*, 2013). The *ZIP12* promoter contains Zn deficiency response elements (ZDRE), placing the gene under the control of the F-group bZIP TFs, and more specifically of bZIP23 (Assunção *et al.*, 2010; Jain *et al.*, 2013; Inaba *et al.*, 2015; Lilay *et al.*, 2019). The activity of ZIP12 upon Zn deficiency was recently shown to be dependent on phosphorylation by calcium-dependent CBL-CIPK (calcineurin B-like-CBL-interacting protein kinases) signaling (Fang *et al.*, 2025).

Unlike most *ZIP* genes, *ZIP12* showed minimal expression in differentiated roots and RT under Zn-limiting conditions (1µM Zn) but was strongly induced upon severe Zn deficiency (0 µM Zn) (**Fig. 6a**), suggesting that it may play a specific role in these conditions. Two *zip12* mutants, *zip12-1* and *zip12-2*, were partially characterized by Inaba *et al.* (2015), both displaying reduced root growth upon Zn deficiency, despite unaltered root Zn levels (Inaba *et al.*, 2015). In our study, only *zip12-1* showed impaired root growth upon Zn deficiency, while *zip12-2* retained strong *ZIP12* expression upon Zn deficiency, consistent with a T-DNA insertion upstream of the 2 ZDREs in the *ZIP12* promoter (**Fig. S1**). In addition, *zip12-1* displayed (i) altered RAM morphology, (ii) constitutive induction of several Zn-responsive *ZIP* genes, (iii) reduced shoot Zn accumulation, (iv) strongly altered Mn and Cu accumulation, (v) elevated Zn level in the vascular cylinder of differentiated roots in control conditions, and (vi) mostly unchanged Zn level in the RAM upon Zn deficiency (**Fig. 7**, **Fig. 4**). Altogether, these findings indicated that *ZIP12* plays an important role in Zn spatialization in the root. We suggest that the strong, constitutive, upregulation of several *ZIP* genes *zip12-1* was responsible for the complex phenotype of the mutant, affecting multiple metals and cell

layers. It was also possibly responsible for the marginal impact of the *zip12-1* mutation on Zn levels in plantlets (this study; Inaba *et al.*, 2015).

According to a recent study by Ochoa Tufiño *et*), *ZIP12* is predominantly expressed in the epidermal cell layer, in the zone connecting the root and the shoot. We showed here that *ZIP12* is also strongly induced by Zn deficiency in the RT (**Fig. 6a**). Moreover, ZIP12 is presumably located to the plasma membrane (Fang *et al.*, 2025). In the *zip12-1* mutant, the concomitant *ZIP12* loss-of-function and up-regulation of *IRT3*, *ZIP4* and *ZIP9* (**Fig. 7d**), which was shown to be involved in Zn radial transport across the root (Lee *et al.*, 2021), may explain both Zn depletion in the epidermis and increased Zn accumulation in the vascular cylinder of differentiated roots (**Fig. 4a, c**). Moreover, the increased Mn accumulation in roots and shoot of the *zip12-1* mutant in control conditions (**Fig. 7e**) may be explained by the upregulation of *ZIP9* (FC ~11 compared to Col-0), encoding a putative Mn transporter (Milner *et al.*, 2013). Why Mn levels were drastically down in *zip12-1* upon Zn deficiency remains to be determined. Increased Mn content upon Zn deficiency in Arabidopsis has been observed previously and was attributed to the regulatory function of the bZIP19 and bZIP23 TFs, potentially via the upregulation of ZIP transporter gene expression (Lilay *et al.*, 2019). In this context, it is interesting to note that neither *ZIP12* nor *ZIP9* are known to be upregulated by Mn deficiency in Arabidopsis (Rodríguez-Celma *et al.*, 2016). Finally, the constitutive upregulation of several *ZIP* genes in *zip12-1*, all with specific cell-type expression patterns (Ochoa Tufiño *et al.*, 2025) and all targets of bZIP19 and bZIP23 (Assunção *et al.*, 2010), suggested that these two TFs may have specific functions, sensing differential Zn status among cell types.

For a long time, knowledge regarding the metal specificity, subcellular localization and overall function of individual ZIP transporters in Arabidopsis has been lagging behind (Ricachenevsky *et al.*, 2015). This mainly stems from the fact that, with a few exceptions (Milner *et al.*, 2013; Inaba *et al.*, 2015), single *zip* mutants typically fail to display strong phenotypes. Recently, the use of multiple mutants has started unveiling the contribution of ZIPs to the Zn uptake pathways in Arabidopsis roots (Lee *et al.*, 2021; Ochoa Tufiño *et al.*, 2025), highlighting the functional redundancy among ZIP transporters. Hence, a quadruple *irt3*, *zip4*, *zip6* and *zip9* mutant is defective in Zn radial transport across the roots, and in consequence displays strongly altered Zn homeostasis and seed development (Lee *et al.*, 2021). A double *zip3*/*zip5* mutant is defective in Zn uptake, while Zn levels are maintained in

the single *zip3* or *zip5* mutants (Ochoa Tufiño *et al.*, 2025). Strikingly, despite its very low expression under Zn-replete and Zn--limiting conditions, but strong induction upon severe Zn deficiency, *ZIP12* emerges as a key actor in the Zn deficiency response. In particular, the fact that a single *zip12* mutant displayed significant alteration in both growth and metal homeostasis points to a pivotal role, with little redundancy, in maintaining root development and nutrient balance upon severe Zn deficiency.

Conclusions

Altogether, this study showed that root growth inhibition upon Zn deficiency may be explained by a reduction of the final size of the mature cells, and a diminution of the number of dividing cells in the division zone of the RT, resulting from accelerated cell elongation and differentiation. We further showed that Zn allocation to the RT is prioritized upon Zn deficiency and identified ZIP12 as a key actor of the response to severe Zn deficiency. As such, this work provides a solid foundation for understanding the complex responses to Zn deficiency in the root tips of Arabidopsis.

Acknowledgments

We thank Prof. Mark Aarts for the kind gift of pZIP4:GUS seeds, as well as A. Degueldre for technical support in ICP-OES analyses. We thank Prof. Stephan Clemens, Prof. Lieven de Veylder, Dr. Ana G.L. Assunção, and Dr. Grmay H. Lilay for helpful discussions. Funding was provided by the “Fonds de la Recherche Scientifique-FNRS” (CDR J.0009.17 to M.H.; PDR-T0120.18, PDR-T.0104.22 to M.H. and N.V.). The authors wish to thank the COST ACTION 19116 PLANTMETALS for efficient networking and discussion. No conflict of interest declared.

Author contributions

MH and NV conceived and directed the research. NT, MH, NV and DPP designed the experiments. NT, DDP, PS, MS, MC, BB and SF performed all experiments. NT, DPP, NV and MH analysed the data. NT made the figures. NT, MH, MS and NV wrote the manuscript, with comments of all authors.

Data availability

The RNA-Seq reads have been deposited in the National Center for Biotechnology Information (NCBI) Sequence Read Archive (SRA) Database with BioProject identification number (submission in progress). The other data that support the findings of this study are available from the corresponding authors upon reasonable request.

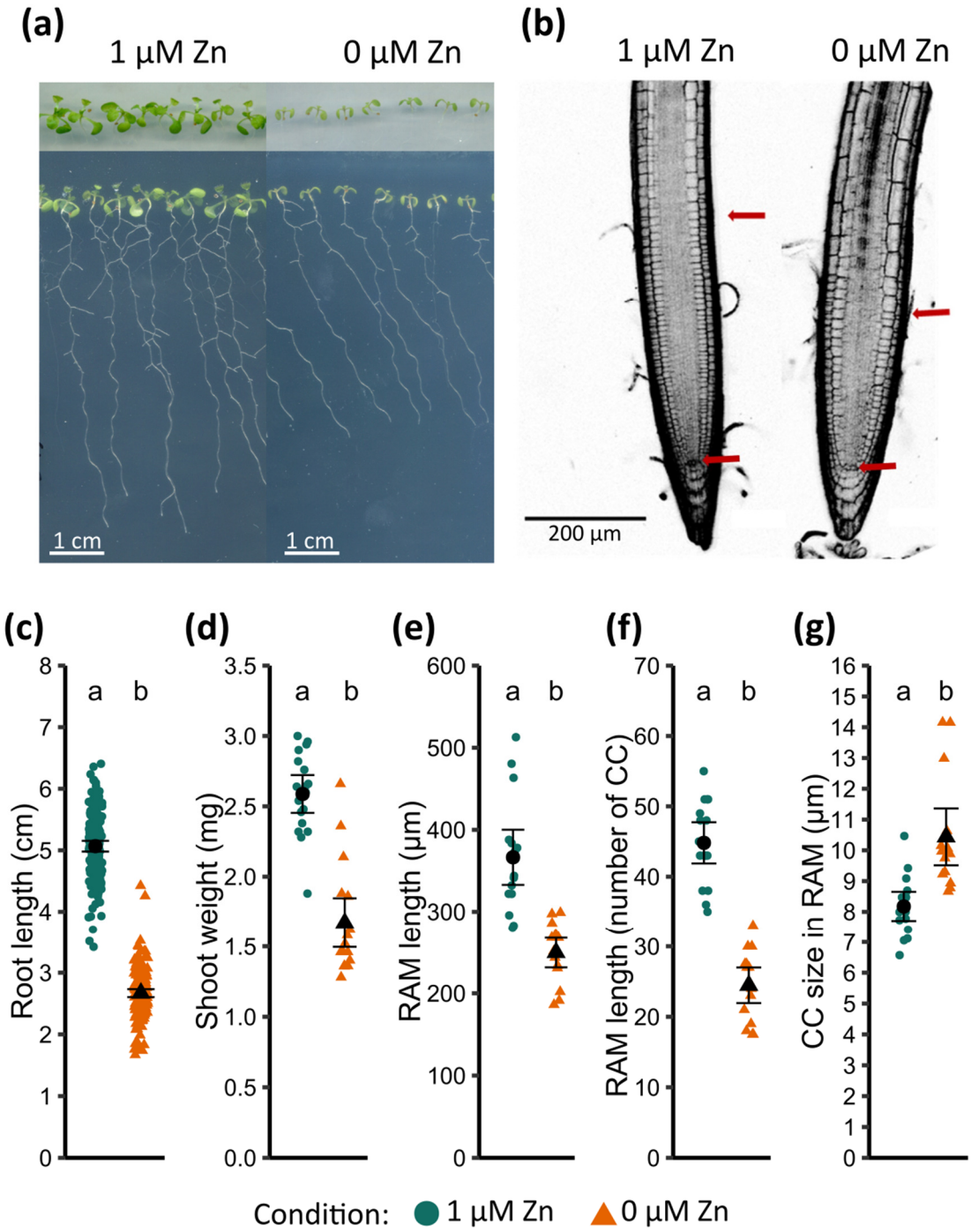

Figure 1. Primary root growth inhibition and impact on the root apical meristem upon Zn deficiency in Arabidopsis. Plantlets were grown for two weeks on EDTA-washed agar plates in control (1 µM Zn) or Zn deficiency (0 µM Zn) conditions. **a.** Representative pictures of the shoots (top) and roots (bottom). **b.** Representative images of root apical meristem (RAM). RAM size was measured between the two red arrows pointing the quiescent center (QC) (lower arrow) and the first elongated cortex cell (upper arrow). **c-d.** Primary root length and shoot

fresh weight, respectively. Values are from 4 independent biological replicates each including 90-96 plantlets per condition. **e-f.** RAM length was assessed both in µm (**e**) and number of cells in the cortex cell layer (**f**). **g.** Mean CC size in the RAM, obtained by dividing the length of RAM by the number of cortex cells for each meristem. **e-g**. Data were pooled from 2 independent experiments (representing 24 individual RAM per condition). **c-g.** Black dots and whiskers represent mean values and standard deviations, respectively. Different letters correspond to statistically different groups (ANOVA type I, *p-value* < 0.05).

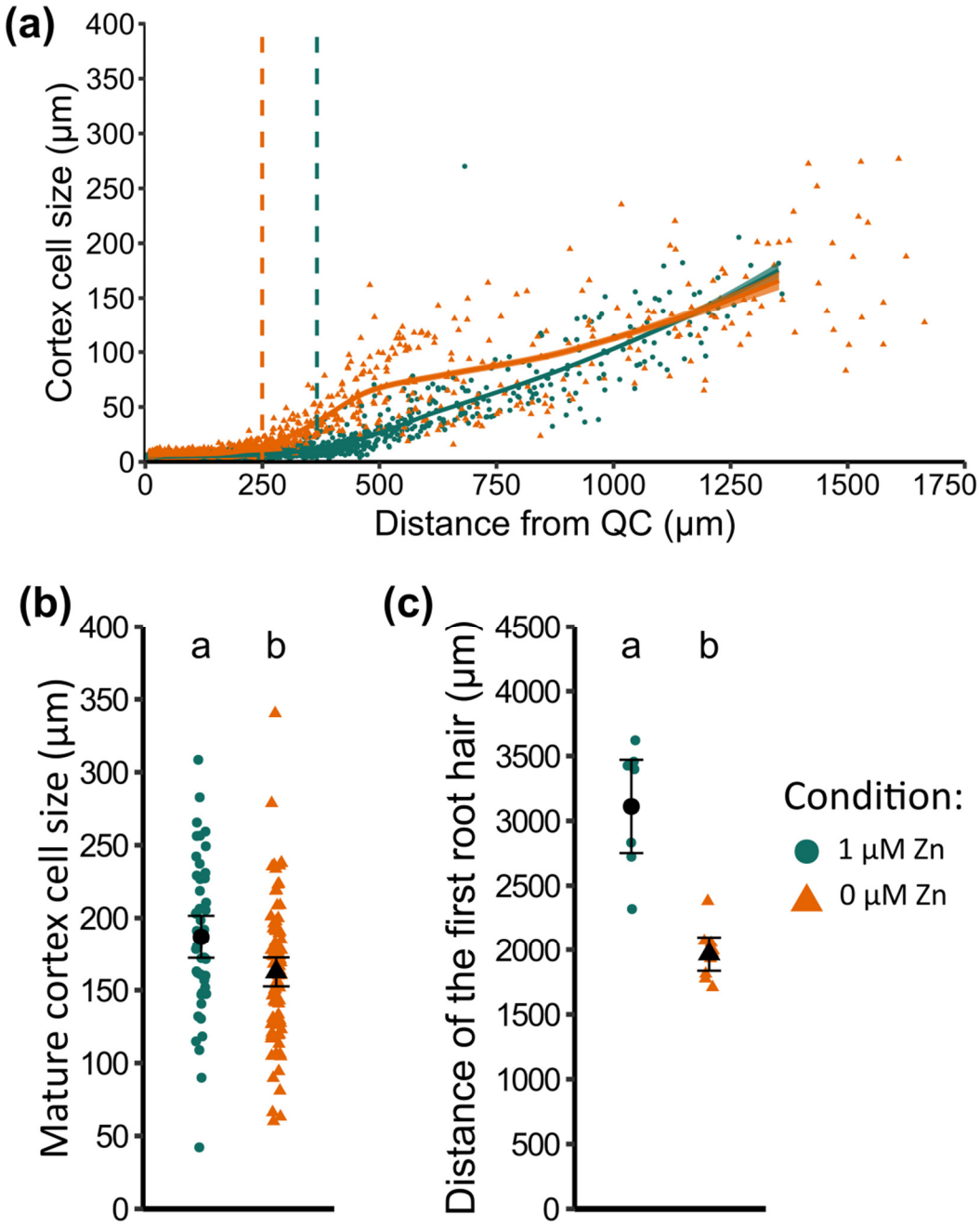

Figure 2. Effect of Zn deficiency on cell elongation. Plantlets were grown for two weeks on EDTA-washed agar plates in control (1 µM Zn) or Zn deficiency (0 µM Zn) conditions. **a.** Distribution of cortex cell size as a function of the distance from the quiescent center (QC). The vertical dashed lines represent the calculated mean RAM size for each condition. The trend lines and SE (standard error) areas were calculated with the "loess" function of ggplot2 R package (x~y) with a SE confidence interval of 0.95, and span of 0.5. **b.** Mean length of mature cortex cells, measured at a distance between 5 and 6 mm from the tip of the root. **a-b**. Data from 2 independent experiments (each 12 individual primary RAM per condition). Either all

717 the visible cortex cells (**a**) or three representative elongated cortex cells were measured
718 between 5 and 6 mm from the QC for each root (**b**). **c**. Elongation zone (EZ) size measured as
719 the distance between the meristem limit and the first root hair. Black dots and whiskers
720 represent mean value and standard deviation, respectively. Different letters correspond to
721 statistically different groups (ANOVA type I, *p-value* < 0.05).
722

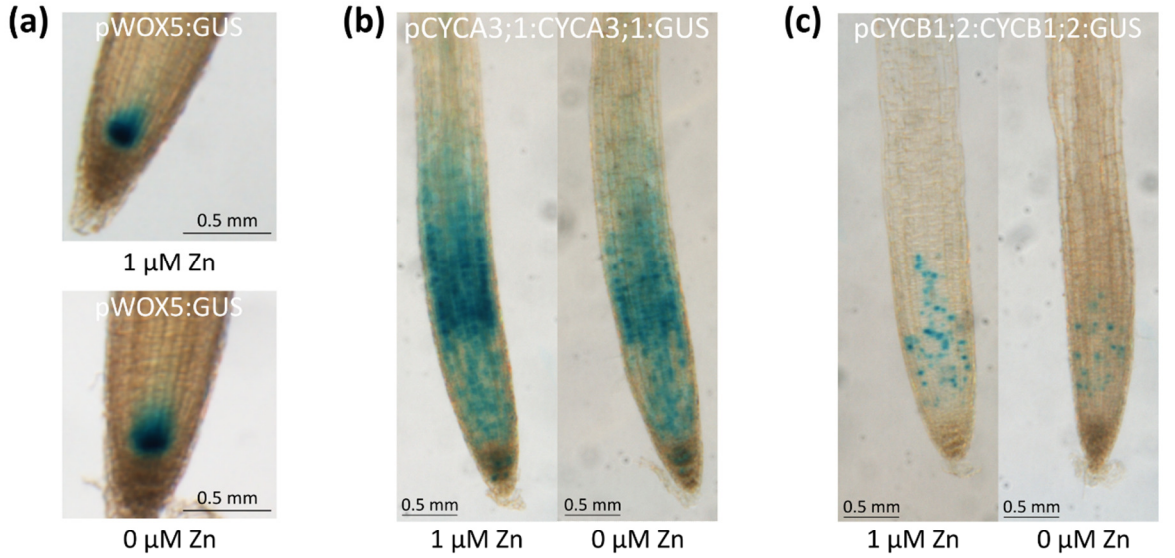

(d)

	pCYCA3;1:CYCA3;1:GUS Enzymatic activity (pmol MU $min^{-1}.mg^{-1}$)	pCYCB1;2:CYCB1;2:GUS Positive spots
1 µM Zn	**272.5** ± 16.35 ^{a}	**44.7** ± 10.6 ^{A}
0 µM Zn	**190.5** ± 19.1 ^{b}	**32.7** ± 9.6 ^{B}

(e)

	pCYCB1;2:CYCB1;2:GUS DRI (per µm)	DRI (per cortex cell)
1 µM Zn	**0.15** ± 0.03 ^{a}	**0.87** ± 0.11 ^{A}
0 µM Zn	**0.12** ± 0.03 ^{a}	**0.90** ± 0.25 ^{A}

Figure 3. Effect of Zn deficiency on the root apical meristem (RAM) activity. Plantlets were grown for two weeks on EDTA-washed agar plates in control (1 µM Zn) or Zn deficiency (0 µM Zn) conditions. **a-c.** Representative GUS staining of pWOX5:GUS (**a**), pCYCB1;2:CYCB1;2:GUS (**b**) and pCYCA3;1:CYCA3;1:GUS (**c**) plantlets. GUS staining was performed in biological triplicates (5 plantlets each) per reporter line and conditions. **d.** Quantification of the GUS activity in the root tips of pCYCA3;1:CYCA3;1:GUS (MUG assay, in biological triplicates with samples each composed of ~100 root tips) and pCYCB1;2:CYCB1;2:GUS (number of GUS spots; 15 plantlets per condition). **e.** Division Rate Index (DRI) for pCYCB1;2:CYCB1;2:GUS root tips (i.e. activity/RAM length), as described in Perilli & Sabatini (2010). **d-e**. Different letters correspond to significantly different groups (ANOVA type I, *p-value* < 0.05).

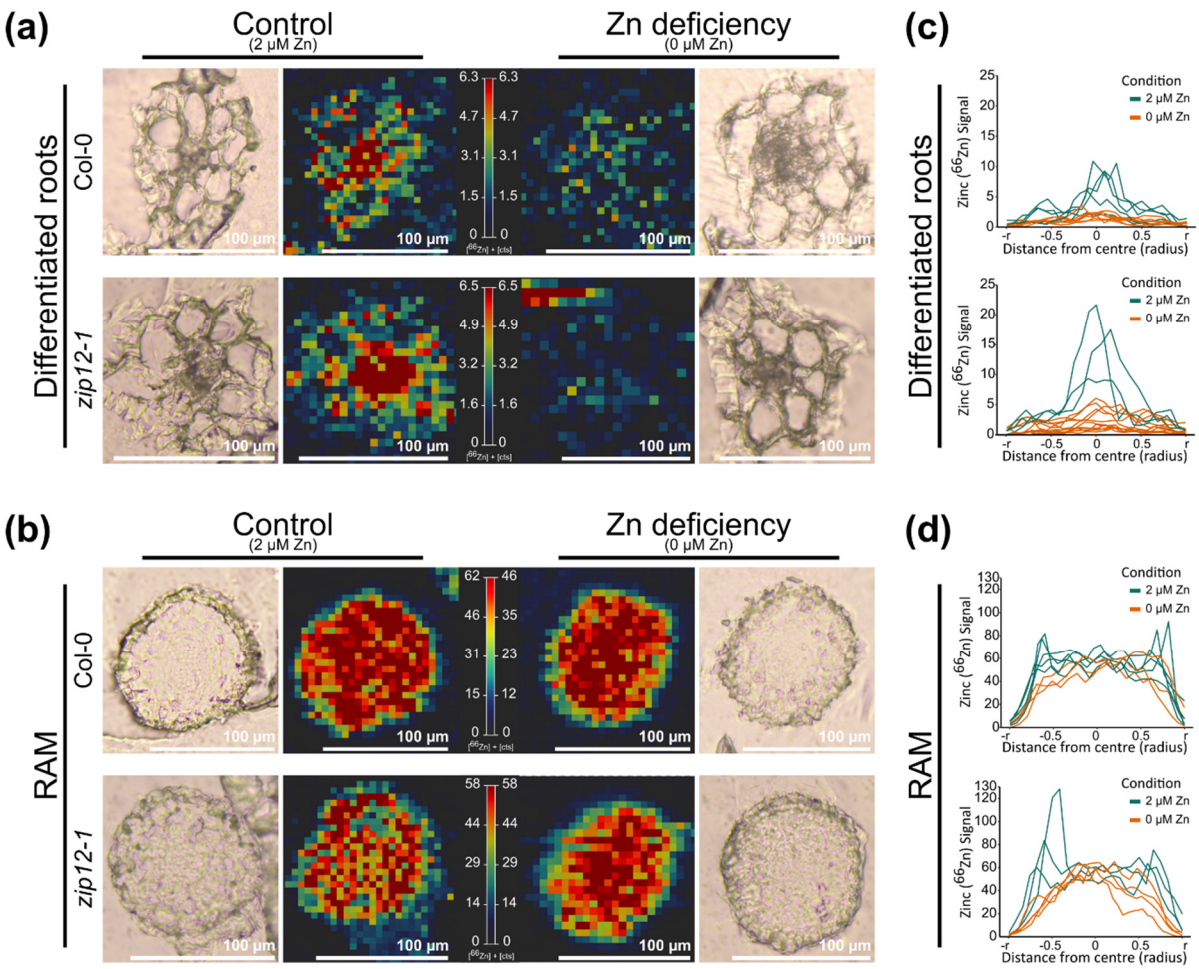

Figure 4. Zn distribution in the root apical meristem (RAM) and differentiated roots upon Zn deficiency in Col-0 and *zip12-1*. Col-0 and *zip12-1* plantlets were grown for two weeks on EDTA-washed agar plates in control (2 µM Zn) or Zn deficiency (0 µM Zn) conditions. Differentiated root (**a, c**) and RAM (**b, d**) transversal sections were then analysed by Laser Ablation ICP-MS. **a-b**. Representative images of the Zn localization. The Zn signal (middle) is surrounded by section optical images (left and right). Laser ablation ICP-MS was conducted on 3 independent replicates of 4 plantlets each, per condition and root part. **c-d**. Intensity graphs representing the Zn signal intensity across individual differentiated roots (**c**) or RAM (**d**) sections. Each graph contains signal from 3-6 well-dried sections, from 3 independently grown plantlets.

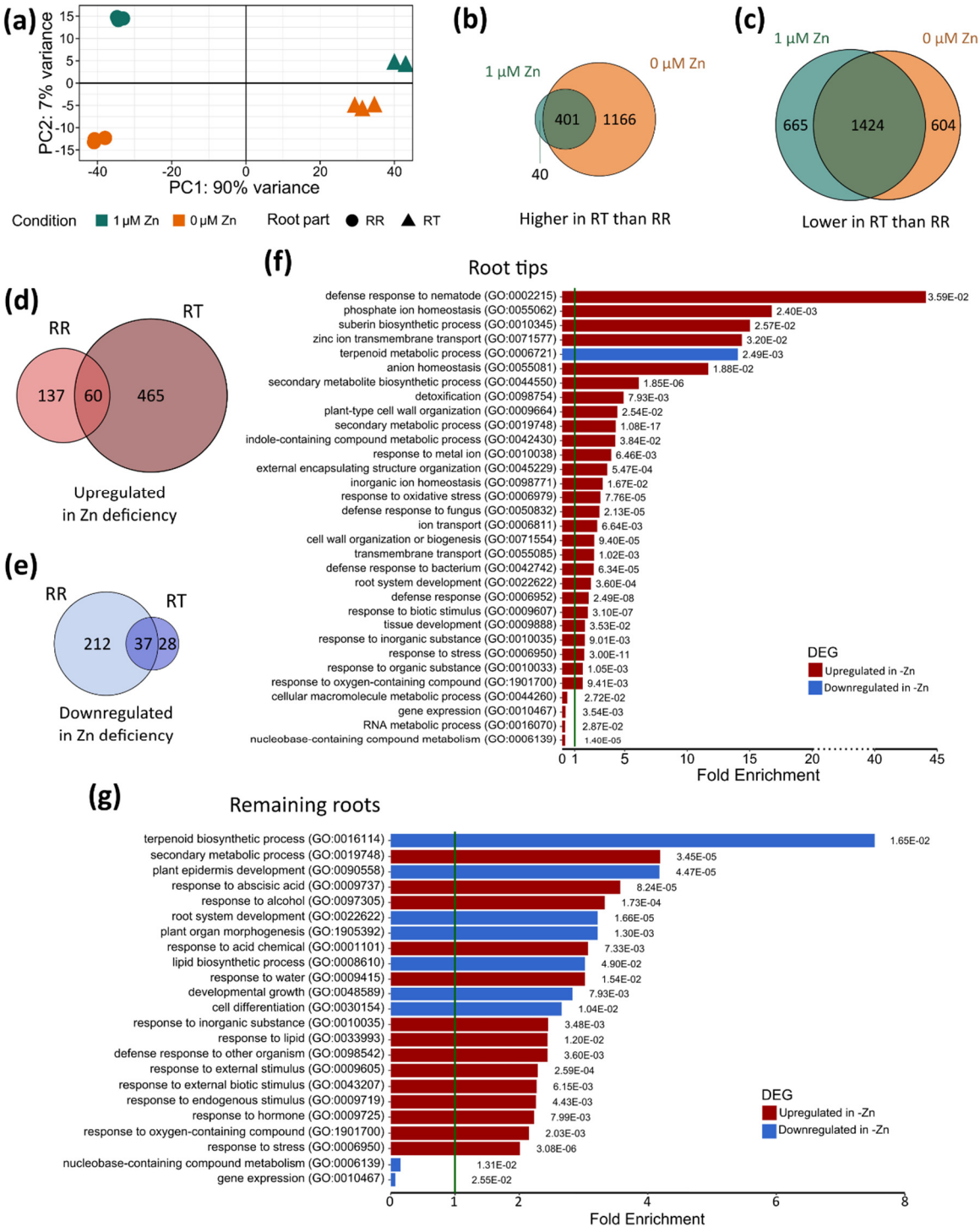

Figure 5. Transcriptome profiling of the root tip and the remaining root system upon Zn deficiency in Arabidopsis. Plantlets were grown in three replicates for two weeks on EDTA-washed agar plates in control (1 µM Zn) or Zn deficiency (0 µM Zn) conditions. **a.** Principal component analysis of the RNA-Seq data. **b-c.** Number of genes that are more (**b**) or less (**c**) expressed in RT than in RR samples in control (green) and Zn deficiency (orange) conditions, respectively. **d-e.** Number of genes that are up- (**d**) or down- (**e**) regulated upon Zn deficiency

compared to the control condition in RT and RR samples, respectively. **b-e**. Differentially expressed genes (DEG) were identified with the following criteria: $\log_2$ (fold change) < -1 of > 1; adjusted *p-value* < 0.05. **f-g.** Representative selection of enriched GO terms among DEGs that are up- or down-regulated upon Zn deficiency in RT (**f**) and RR (**g**). A complete description of the GO enrichment analysis is presented in **Tables S4-S5**.

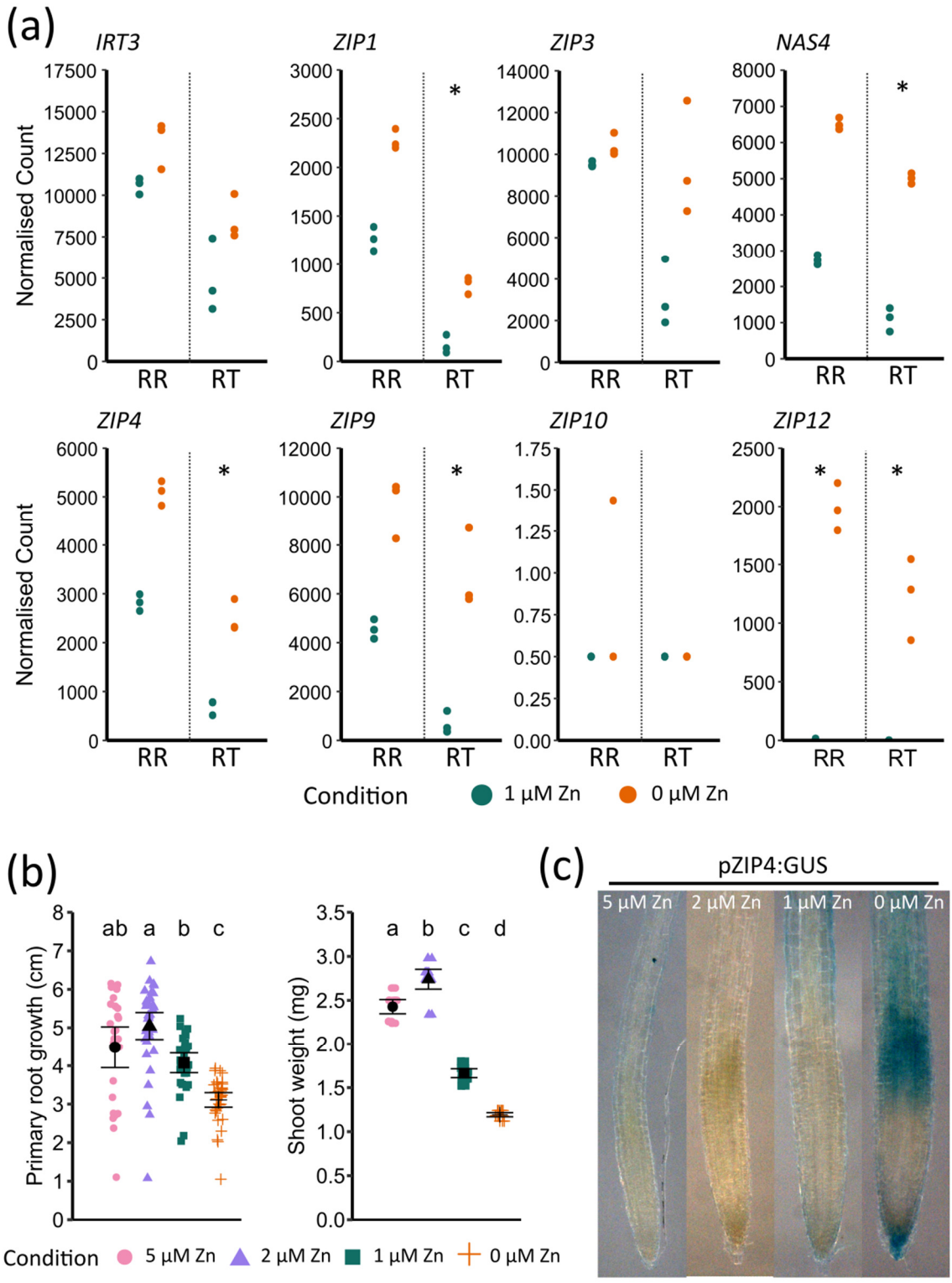

Figure 6. Expression of ZIP transporter genes upon Zn deficiency. Plantlets were grown for two weeks on EDTA-washed agar plates in the presence of different Zn concentrations (5, 2, 1 or 0 µM Zn, as indicated). **a**. Expression of seven ZIP transporter genes from the RNA-Seq analysis. Values are normalized read counts. Stars indicate significantly different expression

between the control (1 µM Zn) and Zn deficiency (0 µM Zn) conditions (log_2(fold change) > 1 , adjusted *p-value* < 0.05). **b**. Primary root growth and shoot fresh weight of Col-0 plantlets. Values are from 3 biological replicates, each including 12 plantlets per condition. Black dots and whiskers represent mean values and standard deviations, respectively. Different letters correspond to statistically different groups (ANOVA type II, with Tukey test correction, *p-value* < 0.05). **c.** GUS staining in primary root apex of pZIP4:GUS plantlets. Pictures are representative of observations made in 10 plantlets.

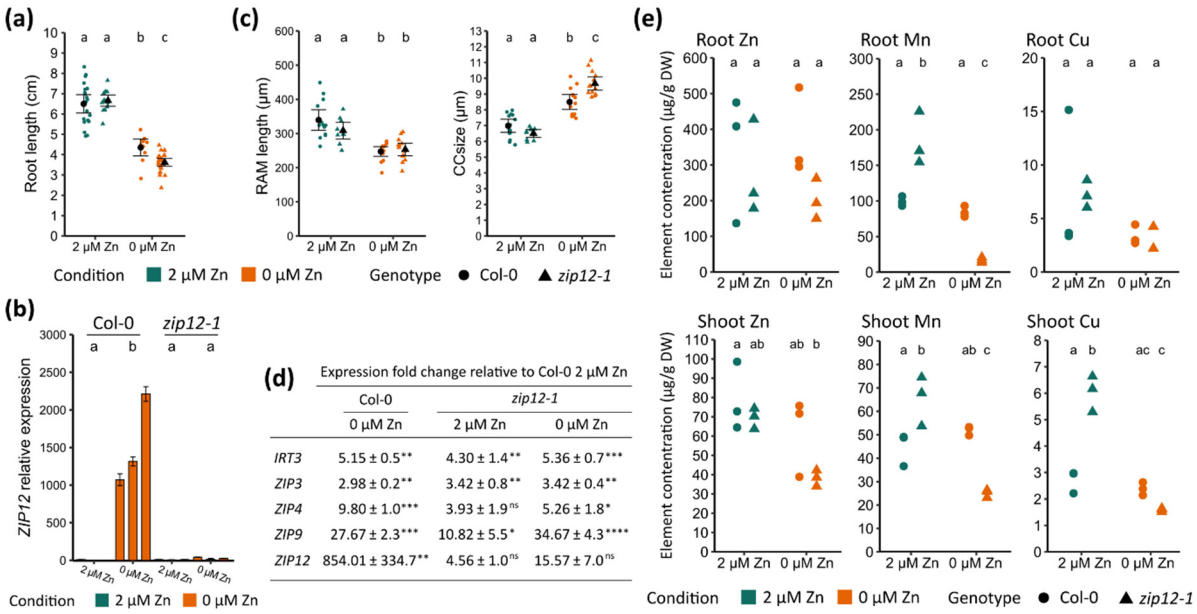

Figure 7. Phenotypes of the *zip12-1* mutant upon Zn deficiency. Plantlets of Col-0 and *zip12-1* were grown for two weeks on EDTA-washed agar plates in control (2 µM Zn) or Zn deficiency (0 µM Zn) conditions. **a.** Primary root length. **b**. *ZIP12* relative expression in Col-0 and *zip12-1* plantlets, as determined by RT-qPCR. Bar values and errors are means +/- SD from 3 technical replicates, normalized on mean expression in Col-0 roots (2 µM Zn). The values for three biological replicates (each including 180 plantlets) are presented. **c.** RAM length and cortex cell size in the RAM of Col-0 and *zip12-1* plantlets. **d.** Summary of the expression of ZIP transporter genes by RT-qPCR, expressed in fold change relative to their expression in roots of Col-0 seedling grown in the presence of 2 µM Zn. Values are from three biological replicates (each including 180 plantlets). Stars correspond to statistically different expression compared to Col-0 roots at 2µM Zn (ANOVA type I, *p-value* < 0.05). **e.** Root and shoot ionome profiling in Col-0 and *zip12-1.* Values are from 3 biological replicates (each including **160-180** plantlets). Different letters represent statistically different groups (ANOVA type II, with Tukey test correction, *p-value* < 0.05).

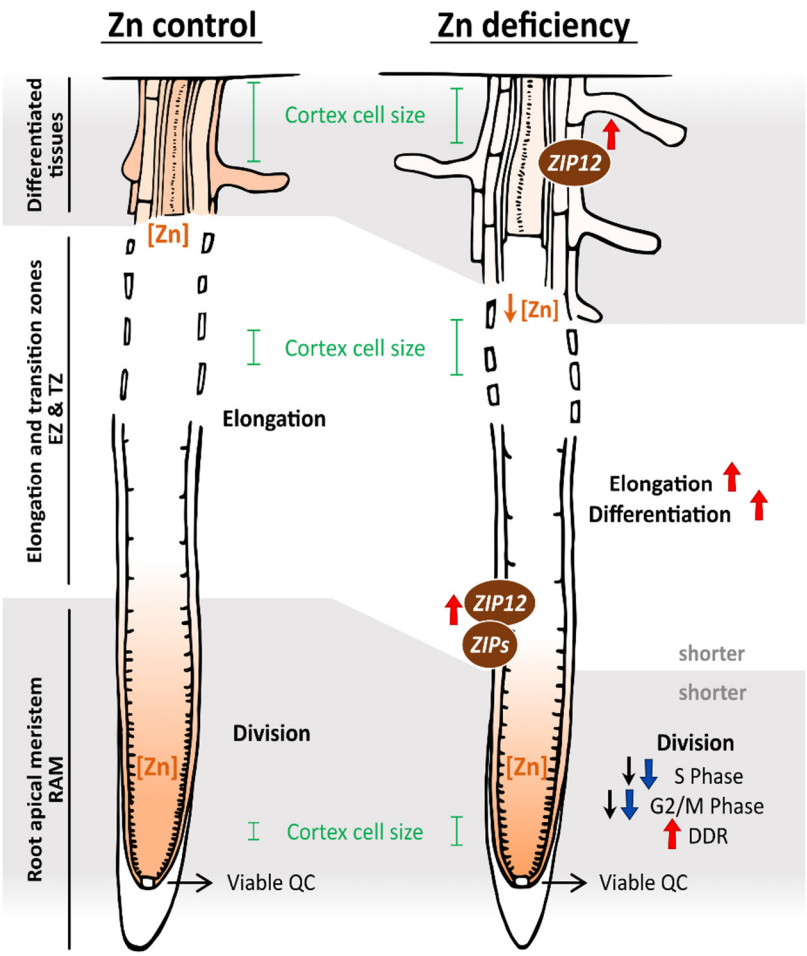

Figure 8. Summary of the response of the RT to Zn deficiency. Under zinc (Zn) deficiency conditions, root apical meristem (RAM) size was reduced, meristematic cortex cells were fewer and longer (**Fig. 1**) with their elongation starting closer to the tip of the root resulting in longer cells in the elongation zone, and differentiation occurring closer to the root apex (**Fig. 2**). Viability and activity of the quiescent centre (QC) and the RAM were maintained, however with fewer individual dividing cells and accelerated elongation (black arrows from GUS activity, red and blues arrows from transcriptomic data, **Figs. 3, 5, Fig. S5**), and with an increased response to DNA damage (DDR) (**Fig. S5**). Zn concentration (orange staining) strongly decreased in differentiated roots, while it was maintained in the RAM, with a slight depletion starting from the external cell layers, especially in the epidermis (**Fig. 4**). Finally, several *ZIP* genes were more expressed in the Zn deficiency roots, especially in the RT, with *ZIP12* being the most upregulated gene in the RT (**Fig. 6, Table 1**). RAM: Root apical meristem. EZ: Elongation zone. DZ: Differentiation zone.

806 **Table 1. Top differentially expressed genes (DEGs) in RT upon Zn deficiency.**

Gene	Gene name	Log_2 (FC) RT	p_{adj}	Log_2 (FC) RR	p_{adj}
Top 10 up-regulated DEGs upon Zn deficiency in RT					
AT5G62160	*ZIP12*	11.76	1.76E-16	7.34	3.88E-76
AT4G28850	*XTH26*	10.28	4.13E-11	1.58	1
AT1G61080	-	9.60	4.50E-10	2.11	0.04
AT3G46340	-	9.60	4.16E-10	0.44	1
AT3G46370	-	9.55	1.14E-09	1.14	1
AT1G51870	-	4	9.61E-09	1.63	1
AT1G34047	*DEFL208*	9.28	2.24E-70	1.55	1
AT3G46410	-	8.51	5.26E-06	3.18	0.29
AT2G29000	-	8.19	2.55E-09	1.38	1
AT5G65980	*PILS7*	8.19	3.6E-07	0.90	1
Top 10 down-regulated DEG upon Zn deficiency in RT					
AT3G60470	-	-7.7	4.66E-06	-1.43	1
AT4G39000	*GH9B17*	-6.54	3.99E-03	-3.54	0.60
AT3G45720	-	-6.42	4.77E-12	-6.18	2.50E-03
AT3G12230	*SCPL14*	-6.29	1.23E-14	-4.35	3.97E-12
AT3G28390	*ABCB18*	-5.82	0.02	-2.67	1
AT4G09780	-	-5.6	1.70E-03	-3.15	2.25E-03
AT3G28380	*ABCB17*	-5.49	2.92E-05	-3.95	1.08E-05
AT1G15610	-	-5.13	1.06E-05	-3.9	8.71E-04
AT1G78440	*ATGA2OX1*	-4.75	2.20E-03	-6.53	1.74E-04
AT3G21670	-	-4.68	2.42E-14	0.93	1
Top 10 up-regulated TF upon Zn deficiency in RT					
AT5G61470	-	6.58	7.10E-04	2.52	0.24
AT3G56970	*bHLH38*	6.56	6.71E-04	2.54	2.55E-03
AT2G25820	*ESE2*	5.91	3.49E-02	2.58	1
AT2G44745	*WRKY12*	5.88	3.27E-02	5.54	7.89E-02
AT4G28800	-	5.51	1.61E-02	0.66	1
AT5G21120	*EIL2*	4.89	4.97E-02	-0.70	1
AT5G62380	*NAC101*	4.57	6.68E-03	-0.17	1
AT3G23250	*MYB15*	4.22	2.58E-14	1.50	1
AT1G74650	*MYB31*	3.97	2.30E-08	1.19	1
AT5G04340	*ZAT6*	3.94	5.07E-16	0.85	1
Down-regulated TF upon Zn deficiency in RT					
AT5G01900	*WRKY62*	-4,25	2,08E-19	-2,17	0,01
AT1G65330	*PHE1*	-3,68	0,02	-4,42	0,37
AT3G57920	*SPL15*	-2,57	0,02	-2,13	0,28
AT2G45660	*AGL20*	-2,19	2,13E-06	-2,69	1,05E-11

807 Gene = Arabidopsis Gene Identifier from the Arabidopsis Genome Initiative, FC= Fold Change between Zn deficient (0 µM Zn)
808 and control (1 µM Zn) samples, p_{adj}= adjusted *p*-value (see Material and Methods): RT= Root Tips, RR=Remaining Root, TF =
809 transcription factor.
810

811

812 **References**

813 **Alloway BJ**. **2008**. Micronutrient deficiencies in global crop production. Springer Science &
814 Business Media.

815 **Amini S, Arsova B, Hanikenne M**. **2022**. The molecular basis of zinc homeostasis in cereals.
816 *Plant, Cell & Environment* **45**: 1339–1361.

817 **Assunção AGL**. **2022**. The F-bZIP-regulated Zn deficiency response in land plants. *Planta* **256**:
818 108.

819 **Assunção AGL, Cakmak I, Clemens S, González-Guerrero M, Nawrocki A, Thomine S**. **2022**.
820 Micronutrient homeostasis in plants for more sustainable agriculture and healthier human
821 nutrition. *Journal of Experimental Botany* **73**: 1789–1799.

822 **Assunção AGL, Herrero E, Lin Y-F, Huettel B, Talukdar S, Smaczniak C, Immink RGH, van Eldik**
823 **M, Fiers M, Schat H, *et al.* 2010**. *Arabidopsis thaliana* transcription factors bZIP19 and bZIP23
824 regulate the adaptation to zinc deficiency. *Proceedings of the National Academy of Sciences*
825 **107**: 10296–10301.

826 **Ayadi A, David P, Arrighi J-F, Chiarenza S, Thibaud M-C, Nussaume L, Marin E**. **2015**. Reducing
827 the genetic redundancy of Arabidopsis PHOSPHATE TRANSPORTER1 transporters to study
828 phosphate uptake and signaling. *Plant Physiology* **167**: 1511–1526.

829 **Barberon M, Vermeer JEM, De Bellis D, Wang P, Naseer S, Andersen TG, Humbel BM,**
830 **Nawrath C, Takano J, Salt DE, *et al.* 2016**. Adaptation of root function by nutrient-induced
831 plasticity of endodermal differentiation. *Cell* **164**: 447–459.

832 **Bhosale R, Boudolf V, Cuevas F, Lu R, Eekhout T, Hu Z, Van Isterdael G, Lambert GM, Xu F,**
833 **Nowack MK, *et al.* 2018**. A spatiotemporal DNA endoploidy map of the Arabidopsis root
834 reveals roles for the endocycle in root development and stress adaptation. *The Plant Cell* **30**:
835 2330–2351.

836 **Bochman ML, Schwacha A**. **2009**. The mcm complex: unwinding the mechanism of a
837 replicative helicase. *Microbiology and Molecular Biology Reviews* **73**: 652–683.

838 **Bouain N, Krouk G, Lacombe B, Rouached H**. **2019**. Getting to the root of plant mineral
839 nutrition: combinatorial nutrient stresses reveal emergent properties. *Trends in Plant Science*
840 **24**: 542–552.

841 **Braidwood L, Breuer C, Sugimoto K**. **2014**. My body is a cage: mechanisms and modulation of
842 plant cell growth. *New Phytologist* **201**: 388–402.

Bulankova P, Akimcheva S, Fellner N, Riha K. **2013**. Identification of Arabidopsis meiotic cyclins reveals functional diversification among plant cyclin genes. *PLOS Genetics* **9**: e1003508.

Cabot C, Martos S, Llugany M, Gallego B, Tolrà R, Poschenrieder C. **2019**. A role for zinc in plant defense against pathogens and herbivores. *Frontiers in Plant Science* **10**: 01171.

Cakmak I. **2000**. Tansley review no. 111 possible roles of zinc in protecting plant cells from damage by reactive oxygen species. *The New Phytologist* **146**: 185–205.

Cakmak I, Kutman UB. **2018**. Agronomic biofortification of cereals with zinc: a review. *European Journal of Soil Science* **69**: 172–180.

Cakmak I, Welch RM, Erenoglu B, Römheld V, Norvell WA, Kochian LV. **2000**. Influence of varied zinc supply on re-translocation of cadmium (109Cd) and rubidium (86Rb) applied on mature leaf of durum wheat seedlings. *Plant and Soil* **219**: 279–284.

Chanfreau GF. **2013**. Zinc'ing down RNA polymerase I. *Transcription* **4**: 217–220.

Chapman EJ, Estelle M. **2009**. Cytokinin and auxin intersection in root meristems. *Genome Biology* **10**: 210.

Charlier J-B, Polese C, Nouet C, Carnol M, Bosman B, Krämer U, Motte P, Hanikenne M. **2015**. Zinc triggers a complex transcriptional and post-transcriptional regulation of the metal homeostasis gene FRD3 in Arabidopsis relatives. *Journal of Experimental Botany* **66**: 3865–3878.

Chen J, Yang L, Yan X, Liu Y, Wang R, Fan T, Ren Y, Tang X, Xiao F, Liu Y, *et al.* 2016. Zinc-finger transcription factor ZAT6 positively regulates cadmium tolerance through the glutathione-dependent pathway in Arabidopsis. *Plant Physiology* **171**: 707–719.

Chesters JK, Petrie L. **1999**. A possible role for cyclins in the zinc requirements during G1 and G2 phases of the cell cycle. *The Journal of Nutritional Biochemistry* **10**: 279–290.

Ciftci-Yilmaz S, Mittler R. **2008**. The zinc finger network of plants. *Cellular and Molecular Life Sciences* **65**: 1150–1160.

Claus J, Bohmann A, Chavarría-Krauser A. **2013**. Zinc uptake and radial transport in roots of *Arabidopsis thaliana*: a modelling approach to understand accumulation. *Annals of Botany* **112**: 369–380.

Clemens S. **2019**. Metal ligands in micronutrient acquisition and homeostasis. *Plant, Cell & Environment* **42**: 2902–2912.

Clemens S. **2022**. The cell biology of zinc. *Journal of Experimental Botany* **73**: 1688–1698.

Cools T, Iantcheva A, Maes S, Van den Daele H, De Veylder L. **2010**. A replication stress-induced synchronization method for *Arabidopsis thaliana* root meristems. *The Plant Journal* **64**: 705–714.

Devaiah BN, Nagarajan VK, Raghothama KG. **2007**. Phosphate homeostasis and root development in Arabidopsis are synchronized by the zinc finger transcription factor ZAT6. *Plant Physiology* **145**: 147–159.

van Dijk JR, Kranchev M, Blust R, Cuypers A, Vissenberg K. **2022**. Arabidopsis root growth and development under metal exposure presented in an adverse outcome pathway framework. *Plant, Cell & Environment* **45**: 737–750.

Domingo G, Locato V, Cimini S, Ciceri L, Marsoni M, De Gara L, Bracale M, Vannini C. **2024**. A comprehensive characterization and expression profiling of defensin family peptides in *Arabidopsis thaliana* with a focus on their abiotic stress-specific transcriptional modulation. *Current Plant Biology* **39**: 100376.

Dong C, He F, Berkowitz O, Liu J, Cao P, Tang M, Shi H, Wang W, Li Q, Shen Z, *et al.* 2018. Alternative splicing plays a critical role in maintaining mineral nutrient homeostasis in rice (*Oryza sativa*). *The Plant Cell* **30**: 2267–2285.

Eekhout T, Larsen P, De Veylder L. **2017**. Modification of DNA checkpoints to confer aluminum tolerance. *Trends in Plant Science* **22**: 102–105.

Esteves SM, Jadoul A, Iacono F, Schloesser M, Bosman B, Carnol M, Druet T, Cardol P, Hanikenne M. **2023**. Natural variation of nutrient homeostasis among laboratory and field strains of *Chlamydomonas reinhardtii*. *Journal of Experimental Botany* **74**: 5198–5217.

Falchuk KH, Fawcett DW, Vallee BL. **1975**. Role of zinc in cell division of *Euglena gracilis*. *Journal of Cell Science* **17**: 57–78.

Fang Y, Ju C, Javed L, Cao C, Deng Y, Gao Y, Chen X, Sun L, Zhao Y, Wang C. **2025**. Plasma membrane-associated calcium signaling modulates zinc homeostasis in Arabidopsis. *Science Bulletin* **70**: 1478–1490.

Fedotova AA, Bonchuk AN, Mogila VA, Georgiev PG. **2017**. C2H2 zinc finger proteins: the largest but poorly explored family of higher eukaryotic transcription factors. *Acta Naturae* **9**: 47–58.

Francis D, Davies MS, Braybrook C, James NC, Herbert RJ. **1995**. An effect of zinc on M-phase and G1 of the plant cell cycle in the synchronous TBY-2 tobacco cell suspension. *Journal of Experimental Botany* **46**: 1887–1894.

Gao S, Xiao Y, Xu F, Gao X, Cao S, Zhang F, Wang G, Sanders D, Chu C. **2019**. Cytokinin-dependent regulatory module underlies the maintenance of zinc nutrition in rice. *New Phytologist* **224**: 202–215.

García MJ, Angulo M, García C, Lucena C, Alcántara E, Pérez-Vicente R, Romera FJ. **2021**. Influence of ethylene signaling in the crosstalk between Fe, S, and P deficiency responses in *Arabidopsis thaliana*. *Frontiers in Plant Science* **12**: 643585.

Garcia V, Bruchet H, Camescasse D, Granier F, Bouchez D, Tissier A. **2003**. *AtATM* is esential for meiosis and the somatic response to DNA damage in Plants. *The Plant Cell* **15**: 119–132.

Garcia-Oliveira AL, Chander S, Ortiz R, Menkir A, Gedil M. **2018**. Genetic basis and breeding perspectives of grain Iron and zinc enrichment in cereals. *Frontiers in Plant Science* **9**: 00937.

Genschik P, Marrocco K, Bach L, Noir S, Criqui M-C. **2014**. Selective protein degradation: a rheostat to modulate cell-cycle phase transitions. *Journal of Experimental Botany* **65**: 2603–2615.

Gruber BD, Giehl RFH, Friedel S, von Wirén N. **2013**. Plasticity of the Arabidopsis root system under nutrient deficiencies. *Plant Physiology* **163**: 161–179.

Gutiérrez-Alanís D, Yong-Villalobos L, Jiménez-Sandoval P, Alatorre-Cobos F, Oropeza-Aburto A, Mora-Macías J, Sánchez-Rodríguez F, Cruz-Ramírez A, Herrera-Estrella L. **2017**. Phosphate starvation-dependent iron mobilization induces CLE14 expression to trigger root meristem differentiation through CLV2/PEPR2 signaling. *Developmental Cell* **41**: 555-570.e3.

Hassan UM, Aamer M, Umer Chattha M, Haiying T, Shahzad B, Barbanti L, Nawaz M, Rasheed A, Afzal A, Liu Y, *et al.* 2020. The critical role of zinc in plants facing the drought stress. *Agriculture* **10**: 396.

Hesketh JE. **1982**. Zinc-stimulated microtubule assembly and evidence for zinc binding to tubulin. *International Journal of Biochemistry* **14**: 983–990.

Hu Z, Cools T, Veylder LD. **2016**. Mechanisms used by plants to cope with DNA damage. *Annual Review of Plant Biology* **67**: 439–462.

Huang H, Ullah F, Zhou D-X, Yi M, Zhao Y. **2019**. Mechanisms of ROS regulation of plant development and stress responses. *Frontiers in Plant Science* **10**: 00800.

Huizinga S, Persson DP, Assunção AGL. **2025**. Constitutive expression of bZIP19 with the Zn sensor motif deleted in Arabidopsis leads to Zn-specific accumulation and no visible developmental penalty. *Plant and Soil* **506**: 787–804.

Hussain D, Haydon MJ, Wang Y, Wong E, Sherson SM, Young J, Camakaris J, Harper JF, Cobbett CS. **2004**. P-type ATPase heavy metal transporters with roles in essential zinc homeostasis in Arabidopsis. *The Plant Cell* **16**: 1327–1339.

Inaba S, Kurata R, Kobayashi M, Yamagishi Y, Mori I, Ogata Y, Fukao Y. **2015**. Identification of putative target genes of bZIP19, a transcription factor essential for Arabidopsis adaptation to Zn deficiency in roots. *The Plant Journal: For Cell and Molecular Biology* **84**: 323–334.

Ireland SM, Martin ACR. **2019**. ZincBind—the database of zinc binding sites. *Database* **2019**: baz006.

Jain A, Poling MD, Smith AP, Nagarajan VK, Lahner B, Meagher RB, Raghothama KG. **2009**. Variations in the composition ofgelling agents affect morphophysiological and molecular responses to deficiencies of phosphate and other nutrients. *Plant Physiology* **150**: 1033–1049.

Jain A, Sinilal B, Dhandapani G, Meagher RB, Sahi SV. **2013**. Effects of deficiency and excess of zinc on morphophysiological traits and spatiotemporal regulation of zinc-responsive genes reveal incidence of cross talk between micro- and macronutrients. *Environmental Science & Technology* **47**: 5327–5335.

Juraniec M, Heyman J, Schubert V, Salis P, De Veylder L, Verbruggen N. **2016**. Arabidopsis *COPPER MODIFIED RESISTANCE1/PATRONUS1* is essential for growth adaptation to stress and required for mitotic onset control. *New Phytologist* **209**: 177–191.

Kanno S, Arrighi J-F, Chiarenza S, Bayle V, Berthomé R, Péret B, Javot H, Delannoy E, Marin E, Nakanishi TM, *et al.* 2016. A novel role for the root cap in phosphate uptake and homeostasis (D Weigel, Ed.). *eLife* **5**: e14577.

Khan GA, Bouraine S, Wege S, Li Y, de Carbonnel M, Berthomieu P, Poirier Y, Rouached H. **2014**. Coordination between zinc and phosphate homeostasis involves the transcription factor PHR1, the phosphate exporter PHO1, and its homologue PHO1;H3 in Arabidopsis. *Journal of Experimental Botany* **65**: 871–884.

Khoso MA, Hussain A, Ritonga FN, Ali Q, Channa MM, Alshegaihi RM, Meng Q, Ali M, Zaman W, Brohi RD, *et al.* 2022. WRKY transcription factors (TFs): Molecular switches to regulate drought, temperature, and salinity stresses in plants. *Frontiers in Plant Science* **13**: 1039329.

Kiba T, Yamada H, Sato S, Kato T, Tabata S, Yamashino T, Mizuno T. **2003**. The type-A response regulator, ARR15, acts as a negative regulator in the cytokinin-mediated signal transduction in *Arabidopsis thaliana*. *Plant and Cell Physiology* **44**: 868–874.

Kimura S, Vaattovaara A, Ohshita T, Yokoyama K, Yoshida K, Hui A, Kaya H, Ozawa A, Kobayashi M, Mori IC, *et al.* 2023. Zinc deficiency-induced defensin-like proteins are involved in the inhibition of root growth in Arabidopsis. *The Plant Journal* **115**: 1071–1083.

Kipreos ET, Pagano M. **2000**. The F-box protein family. *Genome Biology* **1**: reviews3002.1.

Kisko M, Bouain N, Safi A, Medici A, Akkers RC, Secco D, Fouret G, Krouk G, Aarts MG, Busch W, *et al.* 2018. LPCAT1 controls phosphate homeostasis in a zinc-dependent manner (MJ Harrison, Ed.). *eLife* **7**: e32077.

Kong X, Liu G, Liu J, Ding Z. **2018**. The root transition zone: A hot spot for signal crosstalk. *Trends in Plant Science* **23**: 403–409.

Kurz EU, Lees-Miller SP. **2004**. DNA damage-induced activation of ATM and ATM-dependent signaling pathways. *DNA repair* **3**: 889–900.

Lee S, Lee J, Ricachenevsky FK, Punshon T, Tappero R, Salt DE, Guerinot ML. **2021**. Redundant roles of four ZIP family members in zinc homeostasis and seed development in *Arabidopsis thaliana*. *The Plant Journal* **108**: 1162–1173.

Lequeux H, Hermans C, Lutts S, Verbruggen N. **2010**. Response to copper excess in *Arabidopsis thaliana*: Impact on the root system architecture, hormone distribution, lignin accumulation and mineral profile. *Plant Physiology and Biochemistry* **48**: 673–682.

Lešková A, Zvarík M, Araya T, Giehl RFH. **2020**. Nickel toxicity targets cell wall-related processes and PIN2-mediated auxin transport to Inhibit root elongation and gravitropic responses in Arabidopsis. *Plant and Cell Physiology* **61**: 519–535.

Lilay GH, Castro PH, Campilho A, Assunção AGL. **2019**. The Arabidopsis bZIP19 and bZIP23 activity requires zinc deficiency – Insight on regulation from complementation lines. *Frontiers in Plant Science* **9**: 01955.

Lilay GH, Persson DP, Castro PH, Liao F, Alexander RD, Aarts MGM, Assunção AGL. **2021**. Arabidopsis bZIP19 and bZIP23 act as zinc sensors to control plant zinc status. *Nature Plants* **7**: 137–143.

Lilay GH, Thiébaut N, du Mee D, Assunção AGL, Schjoerring JK, Husted S, Persson DP. **2024**. Linking the key physiological functions of essential micronutrients to their deficiency symptoms in plants. *New Phytologist* **242**: 881–902.

Lin Y-F, Hassan Z, Talukdar S, Schat H, Aarts MGM. **2016**. Expression of the *ZNT1* zinc transporter from the metal hyperaccumulator *Noccaea caerulescens* confers enhanced zinc and cadmium tolerance and accumulation to *Arabidopsis thaliana*. *PLOS ONE* **11**: e0149750.

Lin Y-F, Liang H-M, Yang S-Y, Boch A, Clemens S, Chen C-C, Wu J-F, Huang J-L, Yeh K-C. **2009**. Arabidopsis IRT3 is a zinc-regulated and plasma membrane localized zinc/iron transporter. *New Phytologist* **182**: 392–404.

Lindsey BE, Rivero L, Calhoun CS, Grotewold E, Brkljacic J. **2017**. Standardized method for high-throughput sterilization of Arabidopsis seeds. *Journal of Visualized Experiments*: 56587.

Lipka E, Müller S. **2014**. Nitrosative stress triggers microtubule reorganization in *Arabidopsis thaliana*. *Journal of Experimental Botany* **65**: 4177–4189.

Liu S, Strauss S, Adibi M, Mosca G, Yoshida S, Dello Ioio R, Runions A, Andersen TG, Grossmann G, Huijser P, *et al.* 2022. Cytokinin promotes growth cessation in the *Arabidopsis* root. *Current Biology* **32**: 1974-1985.e3.

Lynch JP. **2022**. Edaphic stress interactions: Important yet poorly understood drivers of plant production in future climates. *Field Crops Research* **283**: 108547.

Lynch JP, Strock CF, Schneider HM, Sidhu JS, Ajmera I, Galindo-Castañeda T, Klein SP, Hanlon MT. **2021**. Root anatomy and soil resource capture. *Plant and Soil* **466**: 21–63.

Mager S, Schönberger B, Ludewig U. **2018**. The transcriptome of zinc deficient maize roots and its relationship to DNA methylation loss. *BMC Plant Biology* **18**: 372.

Marrocco K, Bergdoll M, Achard P, Criqui M-C, Genschik P. **2010**. Selective proteolysis sets the tempo of the cell cycle. *Current Opinion in Plant Biology* **13**: 631–639.

Martin RE, Marzol E, Estevez JM, Muday GK. **2022**. Ethylene signaling increases reactive oxygen species accumulation to drive root hair initiation in Arabidopsis. *Development* **149**: dev200487.

Martos S, Gallego B, Cabot C, Llugany M, Barceló J, Poschenrieder C. **2016**. Zinc triggers signaling mechanisms and defense responses promoting resistance to *Alternaria brassicicola* in *Arabidopsis thaliana*. *Plant Science* **249**: 13–24.

Milner MJ, Seamon J, Craft E, Kochian LV. **2013**. Transport properties of members of the ZIP family in plants and their role in Zn and Mn homeostasis. *Journal of Experimental Botany* **64**: 369–381.

van de Mortel JE, Almar Villanueva L, Schat H, Kwekkeboom J, Coughlan S, Moerland PD, Ver Loren van Themaat E, Koornneef M, Aarts MGM. **2006**. Large expression differences in genes for iron and zinc homeostasis, stress response, and lignin biosynthesis distinguish roots of *Arabidopsis thaliana* and the related metal hyperaccumulator *Thlaspi caerulescens*. *Plant Physiology* **142**: 1127–1147.

Moseley JL, Allinger T, Herzog S, Hoerth P, Wehinger E, Merchant S, Hippler M. **2002**. Adaptation to Fe-deficiency requires remodeling of the photosynthetic apparatus. *The EMBO Journal* **21**: 6709–6720.

Nisa M-U, Huang Y, Benhamed M, Raynaud C. **2019**. The Plant DNA Damage Response: Signaling Pathways Leading to Growth Inhibition and Putative Role in Response to Stress Conditions. *Frontiers in Plant Science* **10**.

Nouet C, Charlier J-B, Carnol M, Bosman B, Farnir F, Motte P, Hanikenne M. **2015**. Functional analysis of the three HMA4 copies of the metal hyperaccumulator *Arabidopsis halleri*. *Journal of Experimental Botany* **66**: 5783–5795.

Noulas C, Tziouvalekas M, Karyotis T. **2018**. Zinc in soils, water and food crops. *Journal of Trace Elements in Medicine and Biology* **49**: 252–260.

Ochoa Tufiño V, Almira Casellas M, van Duynhoven A, Flis P, Salt DE, Schat H, Aarts MGM. **2025**. *Arabidopsis thaliana* Zn transporter genes *ZIP3* and *ZIP5* provide the main Zn uptake route and act redundantly to face Zn deficiency. *The Plant Journal* **121**: e17251.

Oteiza PI, Cuellar S, Lönnerdal B, Hurley LS, Keen CL. **1990**. Influence of maternal dietary zinc intake on in vitro tubulin polymerization in fetal rat brain. *Teratology* **41**: 97–104.

Perilli S, Sabatini S. **2010**. Analysis of root meristem size development. In: Hennig L, Köhler C, eds. Plant Developmental Biology: Methods and Protocols. Totowa, NJ: Humana Press, 177–187.

Persson DP, Chen A, Aarts MGM, Salt DE, Schjoerring JK, Husted S. **2016**. Multi-Element Bioimaging of *Arabidopsis thaliana* Roots. *Plant Physiology* **172**: 835–847.

Phukan UJ, Jeena GS, Shukla RK. **2016**. WRKY transcription factors: molecular regulation and stress responses in plants. *Frontiers in Plant Science* **7**: 00760.

Rai V, Sanagala R, Sinilal B, Yadav S, Sarkar AK, Dantu PK, Jain A. **2015**. Iron availability affects phosphate deficiency-mediated responses, and evidence of crosstalk with auxin and zinc in Arabidopsis. *Plant and Cell Physiology* **56**: 1107–1123.

Ramakers C, Ruijter JM, Deprez RHL, Moorman AFM. **2003**. Assumption-free analysis of quantitative real-time polymerase chain reaction (PCR) data. *Neuroscience Letters* **339**: 62–66.

Remans T, Opdenakker K, Guisez Y, Carleer R, Schat H, Vangronsveld J, Cuypers A. **2012**. Exposure of *Arabidopsis thaliana* to excess Zn reveals a Zn-specific oxidative stress signature. *Environmental and Experimental Botany* **84**: 61–71.

Ricachenevsky FK, Menguer PK, Sperotto RA, Fett JP. **2015**. Got to hide your Zn away: Molecular control of Zn accumulation and biotechnological applications. *Plant Science* **236**: 1–17.

Richtmann L, Prochetto S, Thiébaut N, Sarthou MCM, Boutet S, Hanikenne M, Clemens S, Verbruggen N. **2025**. *Arabidopsis thaliana* root responses to Cd exposure: insights into root tip-specific changes and the role of HY5 in limiting Cd accumulation and promoting tolerance. *The Plant Journal* 0.1111/tpj.70298.

Robe K, Barberon M. **2023**. Nutrient carriers at the heart of plant nutrition and sensing. *Current Opinion in Plant Biology* **74**: 102376.

Rodríguez-Celma J, Tsai Y-H, Wen T-N, Wu Y-C, Curie C, Schmidt W. **2016**. Systems-wide analysis of manganese deficiency-induced changes in gene activity of Arabidopsis roots. *Scientific Reports* **6**: 35846.

Sánchez-Calderón L, López-Bucio J, Chacón-López A, Cruz-Ramírez A, Nieto-Jacobo F, Dubrovsky JG, Herrera-Estrella L. **2005**. Phosphate starvation induces a determinate developmental program in the roots of *Arabidopsis thaliana*. *Plant and Cell Physiology* **46**: 174–184.

Sarkar AK, Luijten M, Miyashima S, Lenhard M, Hashimoto T, Nakajima K, Scheres B, Heidstra R, Laux T. **2007**. Conserved factors regulate signalling in Arabidopsis thaliana shoot and root stem cell organizers. *Nature* **446**: 811–814.

Scheepers M, Spielmann J, Boulanger M, Carnol M, Bosman B, De Pauw E, Goormaghtigh E, Motte P, Hanikenne M. **2020**. Intertwined metal homeostasis, oxidative and biotic stress responses in the Arabidopsis *frd3* mutant. *The Plant Journal* **102**: 34–52.

Schnittger A, De Veylder L. **2018**. The dual face of cyclin B1. *Trends in Plant Science* **23**: 475–478.

Shahan R, Hsu C-W, Nolan TM, Cole BJ, Taylor IW, Greenstreet L, Zhang S, Afanassiev A, Vlot AHC, Schiebinger G, *et al.* 2022. A single-cell Arabidopsis root atlas reveals developmental trajectories in wild-type and cell identity mutants. *Developmental Cell* **57**: 543-560.e9.

Shen F, Zhang H, Wan M, Yang Y, Kuang Z, Xiao L, Zuo D, Li Z, Qin G, Li L. **2025**. The CIN-TCP transcription factors regulate endocycle progression and pavement cell size by promoting cell wall pectin degradation. *Nature Communications* **16**: 4108.

Shi L, Lin K, Su T, Shi F. **2023**. Abscisic acid inhibits cortical microtubules reorganization and enhances ultraviolet-B tolerance in *Arabidopsis thaliana*. *Genes* **14**: 892.

Sinclair SA, Krämer U. **2012**. The zinc homeostasis network of land plants. *Biochimica et Biophysica Acta (BBA) - Molecular Cell Research* **1823**: 1553–1567.

Sinclair SA, Senger T, Talke IN, Cobbett CS, Haydon MJ, Krämer U. **2018**. Systemic upregulation of MTP2- and HMA2-mediated Zn partitioning to the shoot supplements local Zn deficiency responses. *The Plant Cell* **30**: 2463–2479.

Sinclair SA, Sherson SM, Jarvis R, Camakaris J, Cobbett CS. **2007**. The use of the zinc-fluorophore, Zinpyr-1, in the study of zinc homeostasis in Arabidopsis roots. *New Phytologist* **174**: 39–45.

Somssich M, Khan GA, Persson S. **2016**. Cell wall heterogeneity in root development of Arabidopsis. *Frontiers in Plant Science* **7**: 01242.

Stanton C, Sanders D, Krämer U, Podar D. **2022**. Zinc in plants: Integrating homeostasis and biofortification. *Molecular Plant* **15**: 65–85.

Stotz HU, Thomson ,James, and Wang Y. **2009**. Plant defensins: Defense, development and application. *Plant Signaling & Behavior* **4**: 1010–1012.

Takahashi H. **2013**. Auxin biology in roots. *Plant Root* **7**: 49–64.

Takahashi N, Kajihara T, Okamura C, Kim Y, Katagiri Y, Okushima Y, Matsunaga S, Hwang I, Umeda M. **2013**. Cytokinins Control Endocycle Onset by Promoting the Expression of an APC/C Activator in *Arabidopsis* Roots. *Current Biology* **23**: 1812–1817.

Takahashi N, Umeda M. **2014**. Cytokinins promote onset of endoreplication by controlling cell cycle machinery. *Plant Signaling & Behavior* **9**: e29396.

Talke IN, Hanikenne M, Krämer U. **2006**. Zinc-dependent global transcriptional control, transcriptional deregulation, and higher gene copy number for genes in metal homeostasis of the hyperaccumulator *Arabidopsis halleri*. *Plant Physiology* **142**: 148–167.

Talukdar S, Aarts MGM. **2008**. *Arabidopsis thaliana* and Thlaspi caerulescens respond comparably to low zinc supply. *Plant and Soil* **306**: 85–94.

Tang W, Luo C. **2018**. Overexpression of zinc finger transcription factor ZAT6 enhances salt tolerance. *Open Life Sciences* **13**: 431–445.

Thiébaut N, Hanikenne M. **2022**. Zinc deficiency responses: bridging the gap between Arabidopsis and dicotyledonous crops. *Journal of Experimental Botany* **73**: 1699–1716.

Thiébaut N, Sarthou M, Richtmann L, Pergament Persson D, Ranjan A, Schloesser M, Boutet S, Rezende L, Clemens S, Verbruggen N, *et al.* 2025. Specific redox and iron homeostasis responses in the root tip of Arabidopsis upon zinc excess. *New Phytologist* **246**: 1796–1815.

Torii K, Kubota A, Araki T, Endo M. **2020**. Time-series single-cell RNA-Seq data reveal auxin fluctuation during endocycle. *Plant and Cell Physiology* **61**: 243–254.

Tsukagoshi H, Busch W, Benfey PN. **2010**. Transcriptional regulation of ROS controls transition from proliferation to differentiation in the root. *Cell* **143**: 606–616.

Urzica EI, Casero D, Yamasaki H, Hsieh SI, Adler LN, Karpowicz SJ, Blaby-Haas CE, Clarke SG, Loo JA, Pellegrini M, *et al.* 2012. Systems and trans-system level analysis identifies conserved iron deficiency responses in the plant lineage. *The Plant Cell* **24**: 3921–3948.

Varshney RK, Barmukh R, Roorkiwal M, Qi Y, Kholova J, Tuberosa R, Reynolds MP, Tardieu F, Siddique KHM. **2021**. Breeding custom-designed crops for improved drought adaptation. *Advanced Genetics* **2**: e202100017.

Velappan Y, Signorelli S, Considine MJ. **2017**. Cell cycle arrest in plants: what distinguishes quiescence, dormancy and differentiated G1? *Annals of Botany* **120**: 495–509.

Veylder LD, Larkin JC, Schnittger A. **2011**. Molecular control and function of endoreplication in development and physiology. *Trends in Plant Science* **16**: 624–634.

Wang H-Y, Klatte M, Jakoby M, Bäumlein H, Weisshaar B, Bauer P. **2007**. Iron deficiency-mediated stress regulation of four subgroup Ib BHLH genes in *Arabidopsis thaliana*. *Planta* **226**: 897–908.

Wang Z, Wang Y, Du Q, Yan P, Yu B, Li W-X, Zou C-Q. **2023**. The auxin signaling pathway contributes to phosphorus-mediated zinc homeostasis in maize. *BMC Plant Biology* **23**: 20.

Ward JT, Lahner B, Yakubova E, Salt DE, Raghothama KG. **2008**. The effect of iron on the primary root elongation of Arabidopsis during phosphate deficiency. *Plant Physiology* **147**: 1181–1191.

Wei P, Demulder M, David P, Eekhout T, Yoshiyama KO, Nguyen L, Vercauteren I, Eeckhout D, Galle M, De Jaeger G, *et al.* 2021. Arabidopsis casein kinase 2 triggers stem cell exhaustion under Al toxicity and phosphate deficiency through activating the DNA damage response pathway. *The Plant Cell* **33**: 1361–1380.

Wessells KR, Brown KH. **2012**. Estimating the global prevalence ofzinc deficiency: Results based on zinc availability in national food supplies and the prevalence of stunting. *PLOS ONE* **7**: e50568.

Wu Y-R, Lin Y-C, Chuang H. **2016**. Laminarin modulates the chloroplast antioxidant system to enhance abiotic stress tolerance partially through the regulation of the defensin-like gene expression. *Plant Science* **247**: 83–92.

Wu X, Wang T, Song H, Jia Y, Ma Q, Tao M, Zhu X, Cao S. **2022**. The transcription factor WRKY12 negatively regulates iron entry into seeds in Arabidopsis. *Journal of Experimental Botany*: erac404.

Xu J, Qin X, Ni Z, Chen F, Fu X, Yu F. **2022**. Identification of Zinc Efficiency-Associated Loci (ZEALs) and Candidate Genes for Zn Deficiency Tolerance of Two Recombination Inbred Line Populations in Maize. *International Journal of Molecular Sciences* **23**: 4852.

Yaqoob U, Jan N, Raman PV, Siddique KHM, John R. **2022**. Crosstalk between brassinosteroid signaling, ROS signaling and phenylpropanoid pathway during abiotic stress in plants: Does it exist? *Plant Stress* **4**: 100075.

Yi C, Wang X, Chen Q, Callahan DL, Fournier-Level A, Whelan J, Jost R. **2021**. Diverse phosphate and auxin transport loci distinguish phosphate tolerant from sensitive Arabidopsis accessions. *Plant Physiology* **187**: 2656–2673.

Zluhan-Martínez E, López-Ruíz BA, García-Gómez ML, García-Ponce B, de la Paz Sánchez M, Álvarez-Buylla ER, Garay-Arroyo A. **2021**. Integrative roles of phytohormones on cell proliferation, elongation and differentiation in the *Arabidopsis thaliana* primary root. *Frontiers in Plant Science* **12**: 659155.

Supporting Information

Table S1. Primers used for the mutant genotyping and RT-qPCR experiments.

Table S2. Expression of marker genes for the cell cycle, endocycle and DDR in the RNA-Seq analysis.

Table S3. Differentially expressed genes (DEGs) between remaining roots (RR) and root tip (RT) samples in control (1 µM Zn) and Zn deficiency (0 µM) conditions.

Table S4. Gene Ontology enrichment analysis amongst the differentially expressed genes (DEGs) less expressed in root tips (RT) than the remaining roots (RR) in control (1 µM Zn) and deficiency (0 µM) conditions.

Table S5. Gene Ontology enrichment analysis amongst the differentially expressed genes (DEG) more expressed in root tips (RT) than remaining roots (RR) in control (1 µM Zn) and deficiency (0 µM) conditions.

Table S6. Differentially expressed genes (DEGs) between control (1 µM Zn) and deficiency (0 µM) conditions in remaining roots (RR) and root tips (RT).

Table S7. Impact of Zn deficiency on developmental processes in root tips (RT) and remaining roots (RR).

Supplementary Figure 1. *zip12* mutant characterization.

Supplementary Figure 2. Comparison of cell elongation rate in the tip of the root in Arabidopsis plantlets grown control (1 µM Zn) or Zn deficiency (0 µM Zn) conditions.

Supplementary Figure 3. Cell cycle synchronization analysis.

Supplementary Figure 4. Illustration of methods.

Supplementary Figure 5. Impact of Zn deficiency on the expression of cell cycle phase, endocycle and DNA damage marker genes in Arabidopsis roots.

Supplemental Figure S6. Impact of Zn deficiency on root tip developmental and mitotic processes.

Supplementary Figure 7. Expression of *ZIP* and *NAS* genes in Arabidopsis roots at various Zn concentrations.

Supplementary Figure 8. Ionome profiling of the roots and shoots in Col-0 and *zip12-1* plantlets upon Zn deficiency.

Methods S1. This section presents detailed Materials and Methods.